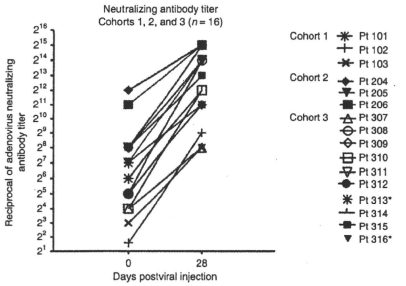

Figure 3 Neutralizing antibody titer. Change in neutralizing antibody titer on day 28 after injection compared to baseline. *Patients 313 and 316 did not have day 28 plasma samples to determine post-treatment neutralizing antibody titer.

housekeeping gene *GAPDH* (glyceraldehyde-3-phosphate dehydrogenase). Tumor hTERT expression was carried out in 12 of 15 tumor biopsies that yielded adequate RNA. Tumor biopsy was not available from pt 316. Endogenous hTERT expression was detected in 9 of the 12 tumor biopsy specimens (**Table 3**). These included two with high hTERT (>10^4 copies/μg) mRNA expression (one in cohort 2 and one in cohort 3), four with moderate expression (10^3–10^4 copies/μg) (one in cohort 1, three in cohort 3), and three with low expression (≤10^3 copies/μg) (one in cohort 1, two in cohort 3). hTERT was below detection limit in three other patients tested (one in cohort 1, two in cohort 3). Of the three patients with prolonged, detectable plasma viral DNA at day 7 post-treatment, pt 205 displayed a high level of endogenous hTERT mRNA, whereas tumor samples were either unavailable (pt 316) or inadequate (pt 312) for assessment. These limited findings confirm hTERT expression in the majority of human tumors.

DISCUSSION

Telomelysin administration in this Phase I safety trial demonstrated safety with no treatment related grade 3/4 adverse effects. Further, we observed the encouraging findings of one patient with partial response at day 56 after a single IT. The transient presence of systemic Telomelysin dissemination following IT was documented early after IT injection. Immune activation was observed, with cytokine upregulation of IL-6 and IL-10 and the induction of viral neutralizing antibodies. Limited suggestive evidence of vial replication was observed at day 7 post-treatment in three patients, for whom plasma viremia was not detected on day 1. One of these three patients had elevated malignant tissue hTERT expression with a significant clinical response. However, these limited findings require additional confirmation as we cannot completely exclude the unlikely possibility of delayed viral clearance. Immunohistochemical analysis of viral E1A and hexon was negative 28 days after injection suggesting rapid clearance. In Galanis' Phase II osteosarcoma trial with ONYX-015, 5 of 6 patients had detectable viral DNA on Day 5 of the first cycle.[7] In Makower's hepatobiliary tumor trial with ONYX-015, no viral DNA was detected in plasma following intralesional injection.[8] In our previous work with ONYX-015 we showed that 41% of patients had detectable viral DNA at days 5 and 6, and 9% had circulating DNA at day 10.

Adenoviral immunogenicity can be affected by viral structural modification (E3 region function), physical properties (temperature), other agents (enbrel, steroids), serotype status, removal of neutralizing antiviral antibodies (plasmapheresis) or presence of antibody producing cells (B-cell inhibition secondary to Ribavirin, Rituxan), use of physical shields (liposome, polymer, cellular delivery), and/or alteration of neutralizing surface epitopes (hexon, knob, fiber).[9–32]

Evidence of clinical efficacy has previously been demonstrated with a *E1B-55* kd deleted oncolytic adenoviral therapeutic (ONYX-015); however, the opportunity to move towards systemic administration was hampered by efficacy results and the limitations imposed by rapid viral clearance and low replication capacity. These data were insufficient for advancement of phase III development with ONYX-015. Telomelysin was designed with a structure to enhance tumor selective viral gene expression (*hTERT* promoter) thereby allowing the opportunity to consider systemic administration in tandem with masked delivery approaches.[33,34] The adenovirus early transcription unit (E3) encodes for polypeptides (14.7 k, 10.4, 14.5),[35–39] which function to directly block tumor necrosis factor–α activation as well as apoptotic pathways shared by tumor necrosis factor–α and *fas*.[38,40,41] The E3 gp19k protein functions to bind and retain MHC class I molecules within the endoplasmic reticulum, thus preventing surface presentation of viral antigens, thereby limiting class I-restricted CTL clearance of virally infected cells.[35,36,42–45] The expression of the E3 gene region products may, therefore, decrease viral clearance, increase the expression of those viral genes that suppress immune recognition and enhance viral replication.[40,46]

In conclusion, both activity and safety of a single injection approach for Telomelysin has been demonstrated. However, despite activity in a subset of patients, limited clinical relevant responses were observed in others. This may be attributed to the single viral treatment administered to each patient. An increase in viral NAb titer in all patients tested is indicative of systemic immune sensitization following IT. We and others have shown previously that systemic viremia can be maintained at 3–6 days after second intravenous or intra-arterial treatments in spite of the presence of high levels of NAb titers and antiviral cytokines.[47,48] Thus repeat intratumoral or intranvenous injection of Telomelysin is a viable treatment option to achieve an improved clinical response. Alternatively, artificial envelopment of Telomelysin with bilamellar cationic liposomes for "stealth" systemic delivery may be applicable for improving systemic pharmacokinetics and coxsackie and adenovirus receptor-independent tropism.[33,34] With these considerations, data support further clinical assessment of a multi treatment schedule.

MATERIALS AND METHODS

Test article. Telomelysin is manufactured at Introgen Therapeutics, Houston, TX. Telomelysin was reconstituted using aseptic technique in a Biocontainment Level 2 ISO Class 5 Biosafety Cabinet.

Study design. This was a dose escalation study in patients with advanced solid tumors. A single IT of virus particles (vp) was administered through a single injection site using a radial method of distribution in order to evenly

distribute material to both peripheral and central sites of growing tumor without removing the needle completely from the tumor. Most of the viral dose was administered at the tumor periphery and at the interface between normal tissue and tumor; prior studies have indicated improved efficacy with this administration approach.[49] Attempts were made to distribute the virus uniformly along the needle tracks by gradually depressing the syringe plunger during withdrawal of the needle. Each patient was enrolled into one of the following cohorts: Cohort 1: 1×10^{10} vp/tumor ($n = 3$); Cohort 2: 1×10^{11} vp/tumor ($n = 3$); Cohort 3: 1×10^{12} vp/tumor ($n = 10$). Patients in cohorts 1 and 2 remained on study for 28 days after injection. Cohort 3 patients were followed until day 56 post-treatment.

Viral DNA was monitored using quantitative PCR (Q-PCR) technique. After the first patient was enrolled into Cohort 1, each of the remaining patients (*i.e.*, pt 2 and pt 3) was enrolled. In Cohort 1, clearance of viral DNA in all body fluid specimens including blood, saliva, sputum, and urine of the preceding patients by two consecutive negative Q-PCR results at least 3 days apart was required. Enrollment of the first patient in Cohort 2 began when viral DNA results on the last patient in Cohort 1 were negative on two consecutive tests at least 3 days apart.

If a dose-limiting toxicity was observed in one of three patients related to Telomelysin, an additional three patients were enrolled. If only one of the six total patients experienced a dose-limiting toxicity, then the dose escalation would be continued to the next cohort. If two or more of the six patients experienced a dose-limiting toxicity, the maximum tolerated dose would be defined as exceeded and an additional three patients would be treated at the dose level below. Toxicities were graded and reported according to the National Cancer Institute common terminology criteria for adverse events, version 3.0. Response was evaluated in this study using the international criteria proposed by the RECIST Committee.

Study population. Patients with superficial accessible cancer who had failed at least one prior therapeutic regimen and for whom effective conventional therapy was not available were eligible for the study. All patients were required to be at least 18 years old, have histologically confirmed carcinoma and a Karnofsky performance status of at least 70%. Inclusion was also predicated on normal laboratory assessment. All patients were required to provide written consent according to local institutional review board–approved guidelines. Women and men of reproductive potential were required to use contraception.

Baseline assessments included: concomitant medications, interval history, physical examination, performance status, tumor assessment, medical laboratory studies, adenoviral NAb, urinalysis, tumor biopsy, viral DNA in blood, saliva, sputum, and urine. Viral plaque forming titer in serum, cytokine levels (IL-6, IL-10, INF-γ). Peripheral blood immunephenotype analyses were performed for Cohort 3 patients.

Assessments were performed using samples collected as follows: plasma viral DNA: pretreatment and at 30 minutes, 1 hour, 3 hours, 6 hours and on days 1, 7, 14, 21, 28, and 56 post-treatment; viral DNA in sputum, urine, and saliva: pretreatment and days 1, 7, 14, 21, 28, and 56 postinjection; endogenous hTERT expression: assessed with pretreatment tumor biopsy; adenovirus NAb: pretreatment and day 28 post-treatment; cytokine: pretreatment and 30 minutes, 1 hour, 6 hours, and on days 1, 14, and 28 post-treatment for first three patients per cohort only; immunohistochemistry for viral hexon: tumor biopsies collected pretreatment and on days 28 and day 56 post-treatment; immunephenotyping analysis: pretreatment and days 7, 14, and 28 post-treatment. Viral plaque assay was performed only on patient plasma samples that yielded $\geq 1 \times 10^5$ vp/ml by Q-PCR analysis.

Detection of viral DNA. Patient samples were collected previral infusion and on day 0 (1 hour, 3 hours, 6 hours post-treatment), day 1, 7, 14, 21, 28, and 56 post-IT. DNA extraction was carried out from patient's archived, frozen tumor biopsy specimen, plasma, sputum, saliva, and urine specimens. Viral DNA was quantified by real-time Q-PCRs. Briefly, DNA was extracted with the Qiagen QIAmp DNA Mini Kit (plasma and saliva samples) or QIAamp Viral RNA Mini Kit (urine and sputum samples). Plasma, saliva, sputum, and urine samples from normal donors were used for protocol validation, with or without "spiking" with known amounts of Telomelysin immediately prior to DNA extraction. Q-PCRs were carried out on the iQ5 Q-thermal cycler (BioRad, Hercules, CA), using Telomelysin-specific primers for the E1A and IRES region and the 2 × Power SYBR Green PCR Master Mix (Applied Biosystems, Foster City, CA). The amounts of detectable viral particles were quantified by extrapolation with a standard curve, generated with serially diluted (1:10) DNA templates with predetermined copy numbers (10 to 1×10^6 copies) of pure Telomelysin viral DNA. A positive response is based on the detection of both IRES- and E1A amplification products with an assay threshold of 4×10^2 vp/ml for plasma and saliva; 1×10^3 vp/ml for urine; 2×10^3 vp/ml for sputum samples for both reactions.

Primer sequences

IRES-Forward 5′-GAT TTT CCA CCA TAT TGC CG
IRES-Reverse 5′-TTC ACG ACA TTC AAC AGA CC
E1A-Forward 5′-CCT GTG TCT AGA GAA TGC AA
E1A-Reverse 5′-ACA GCT CAA GTC CAA AGG TT.

Endogenous hTERT expression in patient tumor. To validate viral replication, real time, quantitative real-time-PCR assays were carried out with total RNA from patient tumor biopsy. Briefly, Q-PCR assays were carried out on iQ5 Q-PCR machine (BioRad), using primers and a TaqMan probe specific to hTERT or GAPDH (Sigma/Proligo, St Louis, MO), and TaqMan Core PCR reagents (Applied Biosystems). Total RNA was extracted with the RNeasy Mini Kit (Qiagen, Valencia, CA). cDNAs were generated according to manufacturer's instructions (RETROscript kit; Ambion, Foster City, CA). PCR standard curves for determination of gene copy number in the reaction template were generated with triplicate reactions, using 1:10, serially diluted samples of either the hTERT or GAPDH PCR amplification products.

Primer sequences

hTERT Forward primer: 5′-GCACTGGCTGATGAGTGTGT-3′
hTERT Reverse primer: 5′- CTCGGCCCTCTTTTCTCTG-3′
hTERT TaqMan probe: 5′-(FAM) TTGCAAAGCATTGGAATCAGA CAGCACT-(TAMRA)-3′
GAPDH Forward primer: 5′-GAAGGTGAAGGTCGTAGTC-3′
GAPDH Reverse primer: 5′-GAAGATGGTGATGGGATTTC-3′
GAPDH TaqMan probe: 5′-(FAM) CAAGCTTCCCGTTCTCAGCC (TAMRA)-3′.

Immunohistochemical analysis. A previously described automated immunoperoxidase staining technique was used to characterize viral protein expression.[50] Briefly, viral E1A and hexon expression was determined with the avidin-biotin-complexed immunoperoxidase reaction (*i*VIEW DAB Detection kit; Ventana Medical Systems, Tucson, AZ) following initial incubation with antibodies specific to viral E1A (prediluted mouse monoclonal adenovirus type 5 E1A antibody, GeneTex, Irvine, CA), or hexon (goat antiadenovirus polyclonal antibody (Millipore, Billerica, MA), using the Ventana 320ES System (Ventana Medical Systems, Tucson, AZ).

Flow cytometric immunophenotype analysis. Peripheral blood immunophenotype analysis was carried by a two color immunofluorescence reaction and flow cytometric analysis as described previously.[50] The frequency distribution of T, B, and NK cell subsets: CD45-FITC/CD14-PE, CD3-FITC/CD19-PE, CD4-FITC/CD8-PE, CD13-FITC [CD16 CD56]-PE (all from BD Biosciences, San Jose, CA) were determined.

Serum cytokine analysis. ELISA assays (R&D Quantikine kits, Minneapolis, MN) were used to quantify patient serum cytokine levels.[50] Serial serum samples were analyzed simultaneously, using cytokine-specific immunoassay reagents. The colorimetric reaction was quantified as a function of optical density absorbance at 450 nm with the correction wavelength set at 540 nm

(SpectraMax 340; Molecular Devices, Sunnyvale, CA). The minimal detectable concentration was as follows: interferon-γ: <16 pg/ml; IL-10: <8 pg/ml; IL-6: <1 pg/ml. The percent increase in cytokine level at any time point post-treatment was determined through comparison with serum harvested before Telomelysin injection. Based on inter- and intra-sample variations, increases in cytokine level of ≥50% over baseline were considered significant.

Antiadenovirus antibodies. Adenovirus-NAb titer in patient plasma samples was measured as a function of blocking human adenovirus infection of 293 cells. Briefly, twofold serially diluted patient plasma samples were added to 293 cells that were infected with Telomelysin virus. The plates were evaluated microscopically for the percentage of cells that lysed in presence of patient plasma samples at 72 and 96 hours postinfection. The adenovirus-NAb titer for a given sample was the highest dilution of the plasma that showed a blocking effect (>60% 293 cells intact and attached as monolayer).

ACKNOWLEDGMENTS

We acknowledge Susan Mill and Brenda Marr for their competent and knowledgeable assistance in the preparation of this manuscript.

REFERENCES

1. Tong AW (2006). Oncolytic Viral Therapy for Human Cancer: Challenges Revisited (review). *Drug Development Research* **66**: 260–277.
2. Taki, M, Kagawa, S, Nishizaki, M, Mizuguchi, H, Hayakawa, T, Kyo, S *et al.* (2005). Enhanced oncolysis by a tropism-modified telomerase-specific replication-selective adenoviral agent OBP-405 ('Telomelysin-RGD'). *Oncogene* **24**: 3130–3140.
3. Lichtenstein, DL and Wold, WS (2004). Experimental infections of humans with wild-type adenoviruses and with replication-competent adenovirus vectors: replication, safety, and transmission. *Cancer Gene Ther* **11**: 819–829.
4. Shay, JW, Zou, Y, Hiyama, E and Wright, WE (2001). Telomerase and cancer. *Hum Mol Genet* **10**: 677–685.
5. Kawashima, T, Kagawa, S, Kobayashi, N, Shirakiya, Y, Umeoka, T, Teraishi, F *et al.* (2004). Telomerase-specific replication-selective virotherapy for human cancer. *Clin Cancer Res* **10**(1 Pt 1): 285–292.
6. Lichtenstein, DL, Toth, K, Doronin, K, Tollefson, AE and Wold, WS (2004). Functions and mechanisms of action of the adenovirus E3 proteins. *Int Rev Immunol* **23**: 75–111.
7. Galanis, E, Okuno, SH, Nascimento, AG, Lewis, BD, Lee, RA, Oliveira, AM *et al.* (2005). Phase I-II trial of ONYX-015 in combination with MAP chemotherapy in patients with advanced sarcomas. *Gene Ther* **12**: 437–445.
8. Makower, D, Rozenblit, A, Kaufman, H, Edelman, M, Lane, ME, Zwiebel, J *et al.* (2003). Phase II clinical trial of intralesional administration of the oncolytic adenovirus ONYX-015 in patients with hepatobiliary tumors with correlative p53 studies. *Clin Cancer Res* **9**: 693–702.
9. Pan, Q, Liu, B, Liu, J, Cai, R, Wang, Y and Qian, C (2007). Synergistic induction of tumor cell death by combining cisplatin with an oncolytic adenovirus carrying TRAIL. *Mol Cell Biochem* **304**: 315–323.
10. Nemunaitis, J, Senzer, N, Sarmiento, S, Zhang, YA, Arzaga, R, Sands, B *et al.* (2007). A phase I trial of intravenous infusion of ONYX-015 and enbrel in solid tumor patients. *Cancer Gene Ther* **14**: 885–893.
11. Lin, E and Nemunaitis, J (2004). Oncolytic viral therapies. *Cancer Gene Ther* **11**: 643–664.
12. Wolff, G, Worgall, S, van Rooijen, N, Song, WR, Harvey, BG and Crystal, RG (1997). Enhancement of *in vivo* adenovirus-mediated gene transfer and expression by prior depletion of tissue macrophages in the target organ. *J Virol* **71**: 624–629.
13. Fisher, KD, Green, NK, Hale, A, Subr, V, Ulbrich, K and Seymour, LW (2007). Passive tumour targeting of polymer-coated adenovirus for cancer gene therapy. *J Drug Target* **15**: 546–551.
14. Fujiwara, T, Urata, Y and Tanaka, N (2007). Telomerase-specific oncolytic virotherapy for human cancer with the hTERT promoter. *Curr Cancer Drug Targets* **7**: 191–201.
15. Fujiwara, T, Urata, Y and Tanaka, N (2008). Diagnostic and therapeutic application of telomerase-specific oncolytic adenoviral agents. *Front Biosci* **13**: 1881–1886.
16. Doronin, K, Toth, K, Kuppuswamy, M, Krajcsi, P, Tollefson, AE and Wold, WS (2003). Overexpression of the ADP (E3-11.6K) protein increases cell lysis and spread of adenovirus. *Virology* **305**: 378–387.
17. Delgado-Enciso, I, Cervantes-García, D, Martínez-Dávila, IA, Ortiz-López, R, Alemany-Bonastre, R, Silva-Platas, CI *et al.* (2007). A potent replicative delta-24 adenoviral vector driven by the promoter of human papillomavirus 16 that is highly selective for associated neoplasms. *J Gene Med* **9**: 852–861.
18. Kim, E, Kim, JH, Shin, HY, Lee, H, Yang, JM, Kim, J *et al.* (2003). Ad-mTERT-delta19, a conditional replication-competent adenovirus driven by the human telomerase promoter, selectively replicates in and elicits cytopathic effect in a cancer cell-specific manner. *Hum Gene Ther* **14**: 1415–1428.
19. Vile, RG and Hart, IR (1993). *In vitro* and *in vivo* targeting of gene expression to melanoma cells. *Cancer Res* **53**: 962–967.
20. Savontaus, MJ, Sauter, BV, Huang, TG and Woo, SL (2002). Transcriptional targeting of conditionally replicating adenovirus to dividing endothelial cells. *Gene Ther* **9**: 972–979.
21. Shirakawa, T, Hamada, K, Zhang, Z, Okada, H, Tagawa, M, Kamidono, S *et al.* (2004). A cox-2 promoter-based replication-selective adenoviral vector to target the cox-2-expressing human bladder cancer cells. *Clin Cancer Res* **10**: 4342–4348.
22. Douglas, JT, Rogers, BE, Rosenfeld, ME, Michael, SI, Feng, M and Curiel, DT (1996). Targeted gene delivery by tropism-modified adenoviral vectors. *Nat Biotechnol* **14**: 1574–1578.
23. Haisma, HJ, Pinedo, HM, Rijswijk, A, der Meulen-Muileman, I, Sosnowski, BA, Ying, W *et al.* (1999). Tumor-specific gene transfer via an adenoviral vector targeted to the pan-carcinoma antigen EpCAM. *Gene Ther* **6**: 1469–1474.
24. Goldman, CK, Rogers, BE, Douglas, JT, Sosnowski, BA, Ying, W, Siegal, GP *et al.* (1997). Targeted gene delivery to Kaposi's sarcoma cells via the fibroblast growth factor receptor. *Cancer Res* **57**: 1447–1451.
25. Miller, CR, Buchsbaum, DJ, Reynolds, PN, Douglas, JT, Gillespie, GY, Mayo, MS *et al.* (1998). Differential susceptibility of primary and established human glioma cells to adenovirus infection: targeting via the epidermal growth factor receptor achieves fiber receptor-independent gene transfer. *Cancer Res* **58**: 5738–5748.
26. Grill, J, Van Beusechem, VW, Van Der Valk, P, Dirven, CM, Leonhart, A, Pherai, DS *et al.* (2001). Combined targeting of adenoviruses to integrins and epidermal growth factor receptors increases gene transfer into primary glioma cells and spheroids. *Clin Cancer Res* **7**: 641–650.
27. Ulasov, IV, Zhu, ZB, Tyler, MA, Han, Y, Rivera, AA, Khramtsov, A *et al.* (2007). Survivin-driven and fiber-modified oncolytic adenovirus exhibits potent antitumor activity in established intracranial glioma. *Hum Gene Ther* **18**: 589–602.
28. Zhang, YA, Nemunaitis, J, Samuel, SK, Chen, P, Shen, Y and Tong, AW (2006). Antitumor activity of an oncolytic adenovirus-delivered oncogene small interfering RNA. *Cancer Res* **66**: 9736–9743.
29. Alonso, MM, Gomez-Manzano, C, Bekele, BN, Yung, WK and Fueyo, J (2007). Adenovirus-based strategies overcome temozolomide resistance by silencing the O6-methylguanine-DNA methyltransferase promoter. *Cancer Res* **67**: 11499–11504.
30. Lamfers, ML, Idema, S, Bosscher, L, Heukelom, S, Moeniralm, S, van der Meulen-Muileman, IH *et al.* (2007). Differential effects of combined Ad5- delta 24RGD and radiation therapy in *in vitro* versus *in vivo* models of malignant glioma. *Clin Cancer Res* **13**: 7451–7458.
31. DeWeese, TL, van der Poel, H, Li, S, Mikhak, B, Drew, R, Goemann, M *et al.* (2001). A phase I trial of CV706, a replication-competent, PSA selective oncolytic adenovirus, for the treatment of locally recurrent prostate cancer following radiation therapy. *Cancer Res* **61**: 7464–7472.
32. Kawakami, K, Takeshita, F and Puri, RK (2001). Identification of distinct roles for a dileucine and a tyrosine internalization motif in the interleukin (IL)-13 binding component IL-13 receptor alpha 2 chain. *J Biol Chem* **276**: 25114–25120.
33. Yotnda, P, Chen, DH, Chiu, W, Piedra, PA, Davis, A, Templeton, NS *et al.* (2002). Bilamellar cationic liposomes protect adenovectors from preexisting humoral immune responses. *Mol Ther* **5**: 233–241.
34. Thompson, DH (2008). Adenovirus in a synthetic membrane wrapper: an example of hybrid vigor? *ACS Nano* **2**: 821–826.
35. Ilan, Y, Droguett, G, Chowdhury, NR, Li, Y, Sengupta, K, Thummala, NR *et al.* (1997). Insertion of the adenoviral E3 region into a recombinant viral vector prevents antiviral humoral and cellular immune responses and permits long-term gene expression. *Proc Natl Acad Sci USA* **94**: 2587–2592.
36. Lee, MG, Abina, MA, Haddada, H and Perricaudet, M (1995). The constitutive expression of the immunomodulatory gp19k protein in E1-, E3- adenoviral vectors strongly reduces the host cytotoxic T cell response against the vector. *Gene Ther* **2**: 256–262.
37. Wold, WS, Hermiston, TW and Tollefson, AE (1994). Adenovirus proteins that subvert host defenses. *Trends Microbiol* **2**: 437–443.
38. Wold, WS, Tollefson, AE and Hermiston, TW (1995). E3 transcription unit of adenovirus. *Curr Top Microbiol Immunol* **199** (Pt 1): 237–274.
39. Bett, AJ, Haddara, W, Prevec, L and Graham, FL (1994). An efficient and flexible system for construction of adenovirus vectors with insertions or deletions in early regions 1 and 3. *Proc Natl Acad Sci USA* **91**: 8802–8806.
40. Wittmann, W, Fabricius, EM, Schneeweiss, U, Schaepe, C, Benedix, A, Weissbrich, C *et al.* (1990). Application of microbiological cancer test to cattle infected with bovine leucosis virus. *Arch Exp Veterinarmed* **44**: 205–212.
41. Horwitz, MS, Tufariello, J, Grunhaus, A and Fejer, G (1995). Model systems for studying the effects of adenovirus E3 genes on virulence in vivo. *Curr Top Microbiol Immunol* **199** (Pt 3): 195–211.
42. Wold, WS and Gooding, LR (1991). Region E3 of adenovirus: a cassette of genes involved in host immunosurveillance and virus-cell interactions. *Virology* **184**: 1–8.
43. Rawle, FC, Tollefson, AE, Wold, WS and Gooding, LR (1989). Mouse anti-adenovirus cytotoxic T lymphocytes. Inhibition of lysis by E3 gp19K but not E3 14.7K. *J Immunol* **143**: 2031–2037.
44. Feuerbach, D and Burgert, HG (1993). Novel proteins associated with MHC class I antigens in cells expressing the adenovirus protein E3/19K. *EMBO J* **12**: 3153–3161.
45. Beier, DC, Cox, JH, Vining, DR, Cresswell, P and Engelhard, VH (1994). Association of human class I MHC alleles with the adenovirus E3/19K protein. *J Immunol* **152**: 3862–3872.
46. Kaplan, JM, Armentano, D, Sparer, TE, Wynn, SG, Peterson, PA, Wadsworth, SC *et al.* (1997). Characterization of factors involved in modulating persistence of transgene expression from recombinant adenovirus in the mouse lung. *Hum Gene Ther* **8**: 45–56.
47. Reid, T, Galanis, E, Abbruzzese, J, Sze, D, Wein, LM, Andrews, J *et al.* (2002). Hepatic arterial infusion of a replication-selective oncolytic adenovirus (dl1520): phase II viral, immunologic, and clinical endpoints. *Cancer Res* **62**: 6070–6079.
48. Nemunaitis, J, Cunningham, C, Tong, AW, Post, L, Netto, G, Paulson, AS *et al.* (2003). Pilot trial of intravenous infusion of a replication-selective adenovirus (ONYX-015) in combination with chemotherapy or IL-2 treatment in refractory cancer patients. *Cancer Gene Ther* **10**: 341–352.
49. Heise, CC, Williams, A, Olesch, J and Kirn, DH (1999). Efficacy of a replication-competent adenovirus (ONYX-015) following intratumoral injection: intratumoral spread and distribution effects. *Cancer Gene Ther* **6**: 499–504.
50. Tong, AW, Nemunaitis, J, Su, D, Zhang, Y, Cunningham, C, Senzer, N *et al.* (2005). Intratumoral injection of INGN 241, a nonreplicating adenovector expressing the melanoma-differentiation associated gene-7 (mda-7/IL24): biologic outcome in advanced cancer patients. *Mol Ther* **11**: 160–172.

Oncogene (2010) 29, 1145–1154

www.nature.com/onc

ORIGINAL ARTICLE

A novel translational approach for human malignant pleural mesothelioma: heparanase-assisted dual virotherapy

Y Watanabe[1,2,3], T Kojima[3], S Kagawa[1,3], F Uno[1,3], Y Hashimoto[2,3], S Kyo[4], H Mizuguchi[5], N Tanaka[3], H Kawamura[2], D Ichimaru[2], Y Urata[2] and T Fujiwara[1,3]

[1]*Center for Gene and Cell Therapy, Okayama University Hospital, Okayama, Japan;* [2]*Oncolys BioPharma, Inc., Minato-ku, Tokyo, Japan;* [3]*Department of Surgery, Okayama University Graduate School of Medicine, Dentistry and Pharmaceutical Sciences, Okayama, Japan;* [4]*Department of Obstetrics and Gynecology, Kanazawa University School of Medicine, Kanazawa, Japan and* [5]*Department of Biochemistry and Molecular Biology, Graduate School of Pharmaceutical Sciences, Osaka University, Osaka, Japan*

Malignant pleural mesothelioma (MPM) is a highly aggressive tumor that is related to asbestos exposure. MPM is characterized by rapid and diffuse local growth in the thoracic cavity, and it has a poor prognosis because it is often refractory to conventional therapy. Although MPM is an extraordinarily challenging disease to treat, locoregional virotherapy may be useful against this aggressive disease because of the accessibility by intrapleural virus delivery. In this study, we show that telomerase-specific, replication-selective adenovirus OBP-301 can efficiently infect and kill human mesothelioma cells by viral replication. Intrathoracic administration of virus significantly reduced the number and size of human mesothelioma tumors intrathoracically implanted into *nu/nu* mice. A high-definition, fluorescence optical imaging system with an ultra-thin, flexible fibered microprobe clearly detected intracellular replication of green fluorescent protein-expressing oncolytic virus in intrathoracically established mesothelioma tumors. As the extracellular matrix (ECM) may contribute to the physiological resistance of a solid tumor by preventing the penetration of therapeutic agents (including oncolytic viruses), we also examined whether the co-expression of heparanase, an endoglucuronidase capable of specifically degrading heparan sulfate, that influences the physiological barrier to macromolecule penetration, can modify the permeability of the ECM, resulting in profound therapeutic efficacy. Co-injection of OBP-301 and a replication-defective adenovirus (Ad-*S/hep*)-expressing heparanase resulted in more profound antitumor effects without apparent toxicity in an orthotopic pleural dissemination model. Our results suggest that intrathoracic dual virotherapy with telomerase-specific oncolytic adenovirus in combination with heparanase-expressing adenovirus may be efficacious in the prevention and treatment of pleural dissemination of human malignant mesothelioma.

Oncogene (2010) **29**, 1145–1154; doi:10.1038/onc.2009.415; published online 23 November 2009

Correspondence: Dr T Fujiwara, Center for Gene and Cell Therapy, Okayama University Graduate School of Medicine, Dentistry and Pharmaceutical Sciences, 2-5-1 Shikata-cho, Okayama 700-8558, Japan. E-mail: toshi_f@md.okayama-u.ac.jp
Received 12 July 2009; revised 23 September 2009; accepted 19 October 2009; published online 23 November 2009

Keywords: telomerase; adenovirus; mesothelioma; heparanase; dual virotherapy

Introduction

Malignant pleural mesothelioma (MPM) is an uncommon neoplasm with an annual estimated incidence of 2000–3000 new cases in the United States (Connelly *et al.*, 1987; Price, 1997). In more than 70% of patients, the origin of the tumor is linked to a history of exposure to asbestos fibers (Chahinian *et al.*, 1982; Chailleux *et al.*, 1988). The use of asbestos in Japan increased rapidly after the 1950s and remained at a high level even as the worldwide use of asbestos decreased substantially after the 1980s, therefore, the mortality rate for MPM is expected to continuously increase in Japan (Murayama *et al.*, 2006). MPM is characterized by progressive local tumor invasion and poor median survival ranging from 9 to 16 months (Ruffie *et al.*, 1989). MPM is notoriously refractory to treatment, and neither surgery nor radiotherapy alone results in increased survival (Ball and Cruickshank, 1990; Rusch *et al.*, 1991). Although many chemotherapeutic regimens have been suggested, a standard treatment strategy for MPM remains elusive (Alberts *et al.*, 1988; Ryan *et al.*, 1998). Therefore, the development of novel therapeutic options is required.

Clinical trials of patients with MPM have established the safety of the intrapleural delivery of replication-deficient adenoviral vectors expressing the suicide gene, herpes simplex thymidine kinase, followed by the administration of ganciclovir, an antiviral drug. Some evidence indicates that this approach induces an effective antitumor immune response (Sterman *et al.*, 1998, 2005; Molnar-Kimber *et al.*, 1998). Moreover, intrapleural interferon-ß gene transfer with a replication-defective adenoviral vector may potentially be a useful approach for the generation of antitumor immune responses in MPM patients (Sterman *et al.*, 2007). A significant obstacle to these approaches is the limited distribution of the non-replicative vectors within the tumor mass, even after direct intratumoral administration. Histopathological analyses have shown that these vectors transduce only a few tumor cells,

despite the successful antitumor responses. Therefore, more efficient strategies for the virus to spread within tumors may be required to increase the clinical benefit.

Replication-selective, tumor-specific viruses present a novel approach for the treatment of neoplastic diseases. These vectors are designed to induce virus-mediated lysis of tumor cells after selective viral propagation within the tumor. Telomerase activation is a critical step in carcinogenesis, and it correlates closely with human telomerase reverse transcriptase (hTERT) expression. We constructed an attenuated adenovirus 5 vector (OBP-301, Telomelysin), in which the hTERT promoter element drives expression of the *E1A* and *E1B* genes linked with an internal ribosome entry site. OBP-301 replicated efficiently and induced marked cell killing in a panel of human cancer cell lines, whereas replication as well as cytotoxicity was highly attenuated in normal human cells lacking telomerase activity (Kawashima *et al*., 2004; Taki *et al*., 2005). In this study, we examined the therapeutic potential of intrapleural delivery of OBP-301 against human MPM tumors intrathoracically implanted into *nu/nu* mice. As the extracellular matrix (ECM) may contribute to the physiological resistance of a solid tumor by preventing the penetration of therapeutic agents (including oncolytic viruses), we also examined whether the co-expression of heparanase, an endoglucuronidase capable of specifically degrading heparan sulfate, that influences the physiological barrier to macromolecule penetration, can modify the permeability of the ECM, resulting in profound therapeutic efficacy.

Results

Expression of CAR and hTERT levels in human mesothelioma cell lines

To examine the biological characteristics of human mesothelioma cells, we first used flow cytometry to determine the cell surface expression of coxsackie and adenovirus receptor (CAR). CAR was expressed in all four cell lines tested, although the expression levels varied (Figure 1b). H2052 and H2452 cells showed low,

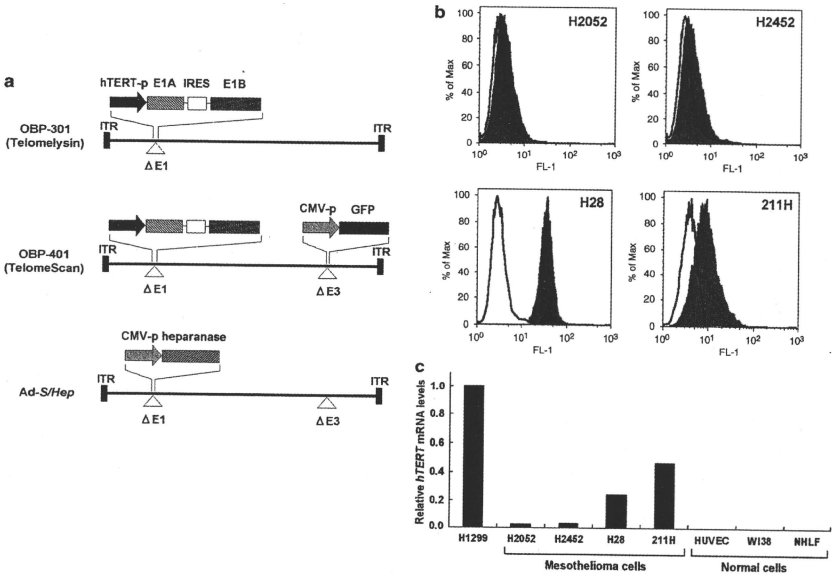

Figure 1 Schematic DNA structures of telomerase-specific viruses and characteristics of human mesothelioma cell lines. (**a**) OBP-301 is a telomerase-specific, replication-competent adenovirus that contains the human telomerase reverse transcriptase (hTERT) promoter sequence inserted into the adenovirus genome to drive transcription of the E1A and E1B bicistronic cassette linked by internal ribosome entry site (IRES). OBP-401 is a variant of OBP-301 and contains the green fluorescent protein *(GFP)* gene inserted under the cytomegalovirus (CMV) promoter into the E3 region for monitoring viral replication. Ad-*S/hep* vector contains human heparanase complementary DNA (cDNA) driven by the CMV promoter. (**b**) Flow cytometric analysis of coxsackie and adenovirus receptor (CAR) expression in human mesothelioma cell lines. Cells were incubated with anti-CAR monoclonal antibodies followed by fluorescein isothiocyanate (FITC)-conjugated rabbit anti-mouse IgG (gray area). An isotype-matched normal mouse IgG conjugated to FITC was used as a control (black line). (**c**) Relative *hTERT* messenger RNA (mRNA) expression in human mesothelioma cell lines and normal cell lines was determined by real-time reverse transcription (RT)–PCR analysis. The *hTERT* mRNA expression of H1299 human lung cancer cells was considered 1.0, and the relative expression level of each cell line was calculated against that of H1299 cells.

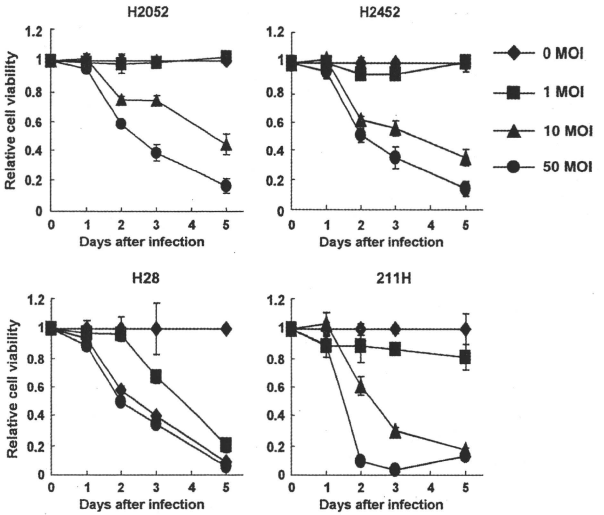

Figure 2 Selective cytopathic effect of OBP-301 in human mesothelioma cell lines *in vitro*. Cells were infected with OBP-301 at the indicated multiplicity of infection (MOI) values, and the surviving cells were quantitated over 5 days by XTT assay. The cell viability of mock-treated cells on day 1 was considered 1.0, and the relative cell viability was calculated. Values represent the mean ± s.d. of triplicate experiments.

but detectable CAR expression compared with CAR-negative cell lines such as LN444, LNZ308 and H1299R5 that we reported earlier (Tango *et al*., 2004; Taki *et al*., 2005). A real-time reverse transcription–PCR method showed that all cell lines expressed detectable levels of *hTERT* messenger RNA (mRNA), suggesting that the hTERT promoter element can be used to target human mesothelioma cells (Figure 1c).

In vitro *cytopathic efficacy of OBP-301 on human mesothelioma cell lines*

To determine whether OBP-301 infection induces selective cell lysis, mesothelioma cells were infected with OBP-301 at various multiplicity of infections (MOIs), and then the XTT cell viability assay was performed over 5 days. All mesothelioma cell lines were efficiently killed by OBP-301 in a dose-dependent manner (Figure 2). Infection at an MOI of 10 was sufficient to induce cell lysis within 3 days. To visually confirm the viral replication and spread, we modified OBP-301 to express the green fluorescent protein (*GFP*) reporter gene under the control of the cytomegalovirus promoter in the E3 region (modified virus, OBP-401) (Figure 1a). We have confirmed earlier that the propagation and yields of OBP-301 and OBP-401 are equivalent (Kawashima *et al*., 2004; Kishimoto *et al*., 2006). After OBP-401 infection, phase-contrast images showed a rapid loss of viability because of massive cell death, as evidenced by ballooning and floating cells. We observed a strong and persistent GFP fluorescence expression in these mesothelioma cells under a fluorescence microscope, indicating the viral replication and spread into the neighboring tumor cells (Figure 3a).

Intrathoracic virus spread and infection in an orthotopic pleural human mesothelioma model

We also evaluated the viral infection and replication in human mesothelioma cells growing intrathoracically in athymic *nu/nu* mice. When H2052 and H2452 mesothelioma cells were inoculated into the thoracic space, disseminated tumor nodules were detected in the visceral pleura, parietal pleura, diaphragmatic pleura and mediastinum. We used H2452 cells with low CAR and *hTERT* mRNA expression that were considered to be most refractory to OBP-301 for the further *in vivo* experiments. Tumor weights at autopsy more than 40 days after tumor cell inoculation were significantly greater than tumor weights at <30 days, indicating the tumor growth in the thoracic cavity (Supplementary Figure 1). Optical charged-coupled device imaging detected GFP-labeled tumors at the gross level during a midsternal thoracotomy 6 days after intrathoracic injection of 1×10^8 plaque-forming units (PFU) of OBP-401. Moreover, GFP expression in macroscopically invisible tumors could be detected at the microscopic level with a hand-held flexible probe inserted through

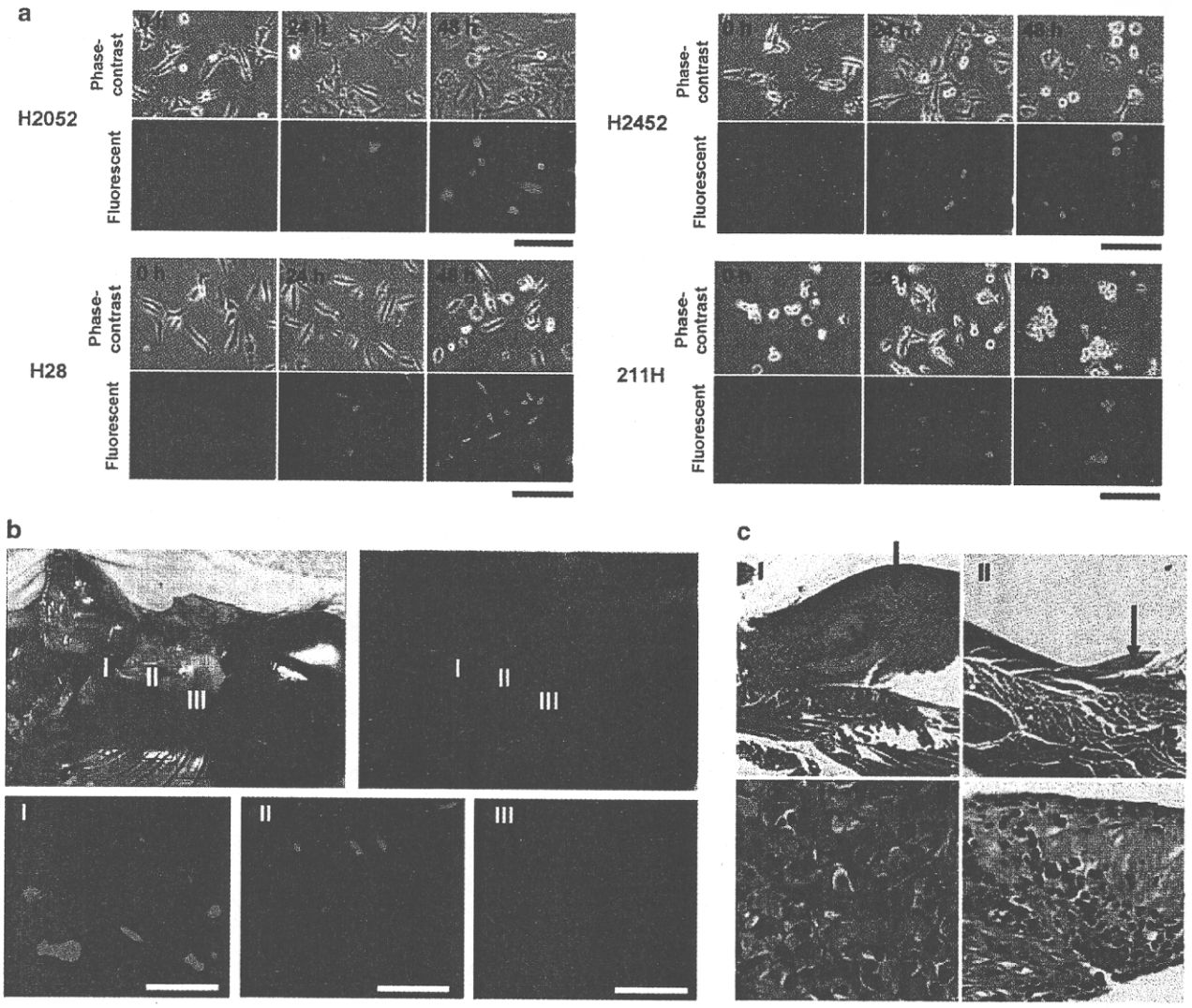

Figure 3 Visualization of human mesothelioma cells *in vitro* and *in vivo* by OBP-401 infection. (**a**) H2052, H2452, H28 and 211 H cells were infected with OBP-401 at an multiplicity of infection (MOI) of 10. Cell morphology and green fluorescent protein (GFP) expression were evaluated by fluorescence microscopy at the indicated time. Bar = 200 μm. (**b**) Internal images of pleural mesothelioma dissemination visualized by intrathoracic injection of OBP-401. Six weeks after intrathoracic inoculation of 5×10^6 H2452 cells, mice received an intrathoracic injection of 1×10^8 plaque-forming units (PFU) of OBP-401. The GFP fluorescence expression was detected 6 days after virus administration by a 3-charged-coupled device (CCD) camera (top panels) and an *in situ* molecular imaging system (bottom panels). Top-left panel, gross appearance of disseminated H2452 tumors; top-right panel, fluorescent detection. Bottom panels, I, II and III represent the boxed regions of the top panels. Bar = 30 μm. (**c**) Histologic sections stained with hematoxylin and eosin showing local growth of H2452 mesothelioma cells (arrows) in the thoracic spaces. Top panels, × 40 magnification; bottom panels, × 400 magnification. I and II represent the boxed regions of (**b**).

the intercostal small incision (Figure 3b and Supplementary Figure 2). Histological analysis confirmed the presence of disseminated tumors in the sites of fluorescence emission (Figure 3c). These results suggest that intrathoracically injected oncolytic virus can infect and selectively replicate in disseminated tumor tissues.

In vivo *antitumor effect of intrathoracic delivery of OBP-301 in an orthotopic pleural human mesothelioma model*
To examine the therapeutic effect of telomerase-specific oncolytic virus, mice received an injection of 1×10^7 or 1×10^8 PFU of OBP-301, 1×10^8 PFU of replication-defective control adenovirus (dl312), or phosphate-buffered saline into the thoracic spacethe injections were administered twice at a 1-week interval beginning 24 h after tumor cell inoculation. Injection of 10^8 PFU of OBP-301 significantly reduced the incidences of tumor cell dissemination and the total weights of tumor nodules as compared with mice that received dl312 or phosphate-buffered saline injection, although 10^7 PFU of OBP-301 had no apparent effect (Figures 4a and b). Next, we examined treatment schedules with different starting points. Two injections of 1×10^8 PFU of OBP-301 administered at a 1-week interval starting on day 1, 8, 22 or 29 after tumor inoculation showed statistically significant antitumor effects when mice were killed on day 43 (Figure 4c and Supplementary Figure 3). These results suggest that oncolytic virotherapy could be

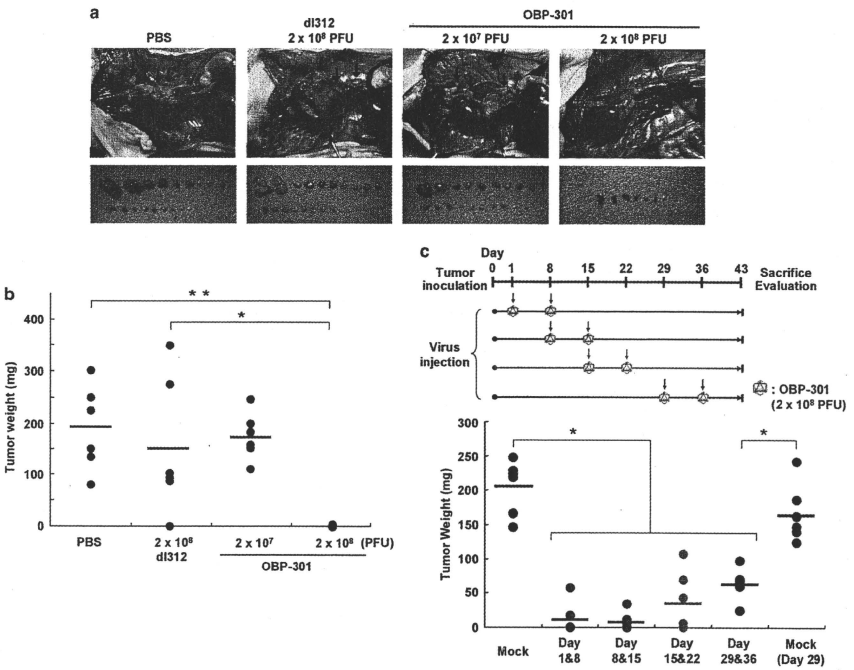

Figure 4 *In vivo* antitumor effect of OBP-301 on pleural dissemination of H2452 human mesothelioma cells. (**a**) Gross appearance of H2452 tumors grown orthotopically in the thoracic spaces. H2452 cells (5×10^6) were inoculated into the thoracic space of athymic *nu/nu* mice. After 24 h, either 1×10^7 plaque-forming units (PFU)/100 µl or 1×10^8 PFU/100 µl of OBP-301, 1×10^8 PFU/100 µl of dl312 (replication-deficient adenovirus), or phosphate-buffered saline (PBS) were injected into the thoracic space twice at a 1-week interval (total dose: 2×10^7 or 2×10^8 PFU). Eight weeks after tumor cell inoculation, the mice were killed, and the pleural dissemination of the thoracic spaces was assessed. (**b**) The weight of each tumor nodule found in the thoracic spaces was determined. Closed circles: individual tumor weights. Bars: mean weight. $*P<0.05$, $**P<0.01$. (**c**) The antitumor effect of OBP-301 administered in different treatment schedules was also assessed on an orthotopic pleural dissemination model. Top panel, treatment schedule. Bottom panel, tumor weight of each tumor nodule found in the thoracic spaces after treatment. The treated mice were killed and assessed for pleural dissemination 43 days after tumor inoculation. Closed circles: individual tumor weights. Bars: mean weight. $*P<0.05$.

effective for preventing the dissemination of mesothelioma cells as well as shrinking established tumors; complete eradication of disseminated nodules, however, was not achieved.

Enhanced antitumor effect of OBP-301 in combination with heparanase-expressing adenovirus in an orthotopic pleural human mesothelioma model

To further enhance the *in vivo* therapeutic potential of telomerase-specific virotherapy, we examined the combination effect of OBP-301 and a replication-defective adenovirus vector expressing the human *heparanase* gene (Ad-*S/hep*) (Uno *et al*., 2001). Heparan sulfate is a major constituent of the ECM that is responsible for a barrier to macromolecular diffusion in tumors. Thus, heparanase-mediated ECM degradation may be a critical requisite for virus penetration and distribution into tumor tissues. Western blot analysis revealed the expression of both proheparanase (*Mr* 65 000) and cleaved, active heparanase (*Mr* 50 000) in H2542 cells after Ad-*S/hep* infection expression of these proteins was not affected by the presence of OBP-301 (Figure 5a). In addition, an *in vitro* XTT analysis showed that co-infection of Ad-*S/hep* at various MOIs did not affect OBP-301-mediated cytotoxicity on human mesothelioma cells (Supplementary Figure 4).

We next examined whether heparanase expression enhanced the virus penetration into three-dimensional tumor structures using a human mesothelioma spheroid model. Tumor spheroids provide an excellent *in vitro* three-dimensional model resembling *in vivo* tumor masses for visualizing the dynamics of the virus and

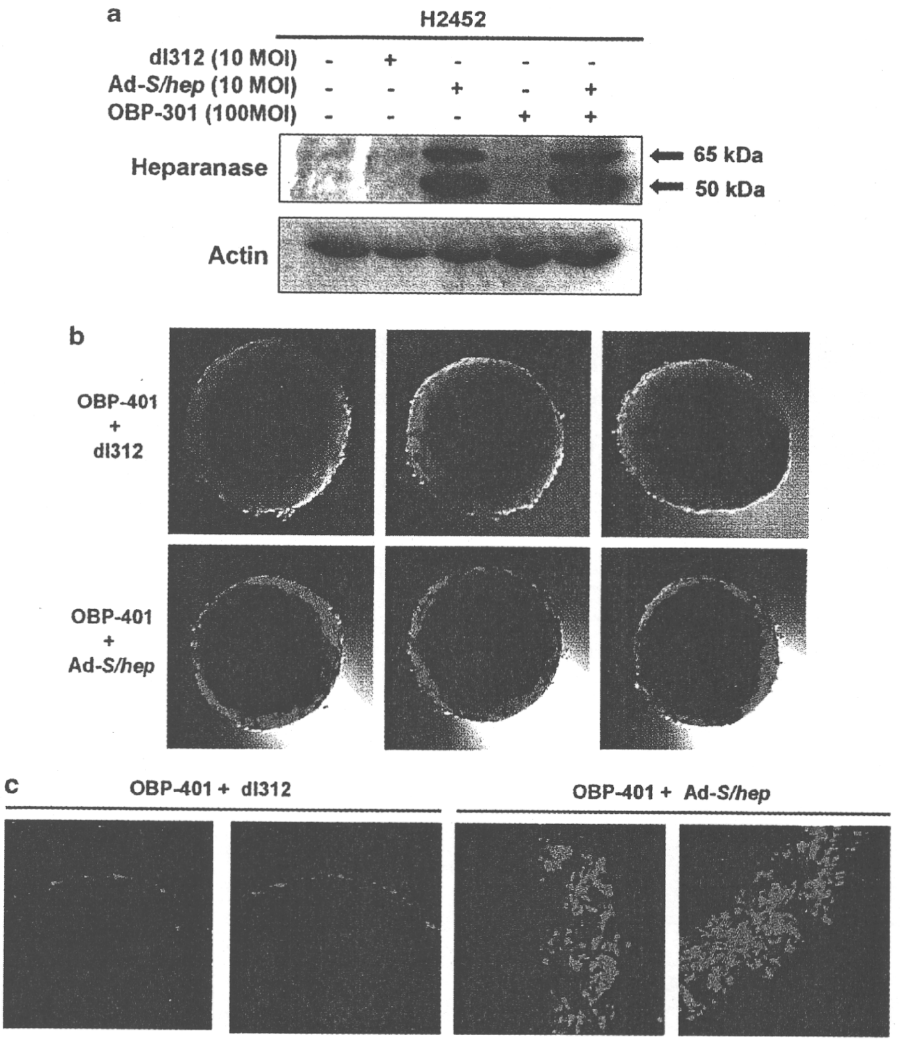

Figure 5 Enhanced penetration of the virus into tumor spheroids by heparanase expression. (**a**) Western blot analysis of human heparanase protein expression in H2452 cells. Cells were infected with either dl312, Ad-*S/hep*, OBP-301 or OBP-301 in combination with Ad-*S/hep* at different multiplicity of infections (MOIs), as indicated. Equivalent amounts of protein obtained from whole cell lysates 30 h after infection were separated by electrophoresis, probed with primary antibodies, and then visualized by using an ECL detection system. Equal loading of samples was confirmed by reprobing with anti-actin antiserum. Both inactive (*Mr* 65 000) and active (*Mr* 50 000) forms of heparanase proteins were detected. (**b**, **c**) Transduction efficiency and viral spread of OBP-401 in combination with Ad-*S/hep* in H2452 tumor spheroids. H2452 tumor spheroids were infected with dl312 (replication-deficient adenovirus) or Ad-*S/hep* at 1×10^3 plaque-forming units (PFU), followed by infection with OBP-401 at 1×10^4 PFU 48 h later. Green fluorescent protein (GFP) expression in each tumor spheroid was assessed with a laser-scanning confocal fluorescent microscope 48 h later. (**b**) Gross imaging of H2452 tumor spheroids. (**c**) Higher magnification to show the surface area of the spheroids.

assessing the levels of virus penetration. Sequential confocal fluorescent microscopy showed that OBP-401 could penetrate and express GFP fluorescence in H2452 spheroids; GFP expression, however, could be detected in the deeper areas of the spheroids in the presence of Ad-*S/hep* (Figure 5b, c). High-magnification images showed that GFP signals were detected only at the spheroid surface after OBP-401 and control dl312 exposure, whereas co-infection of Ad-*S/hep* enhanced the OBP-401 penetration, leading to GFP expression in multiple layers.

Finally, we assessed the combination effect of OBP-301 and Ad-*S/hep* in an orthotopic pleural human mesothelioma model. Intrathoracic injection with 1×10^8 PFU of OBP-301 plus 1×10^7 PFU of Ad-*S/hep* on days 8 and 15 resulted in a significant reduction of tumor weights on day 43 (Figure 6a). This combination therapy showed greater antitumor effects than the therapy with 10^8 PFU of OBP-301 alone. The administration of Ad-*S/hep* alone did not affect tumor weights as compared with the tumors in the mock-treated group. Moreover, only one of the seven (14.3%) mice injected with OBP-301 alone survived over a 12-week observation period, whereas five of the seven (71.4%) mice treated with OBP-301 plus Ad-*S/hep* remained alive (Figure 6b).

Discussion

Malignant pleural mesothelioma is an aggressive neoplasm with a dismal prognosis because of its resistance

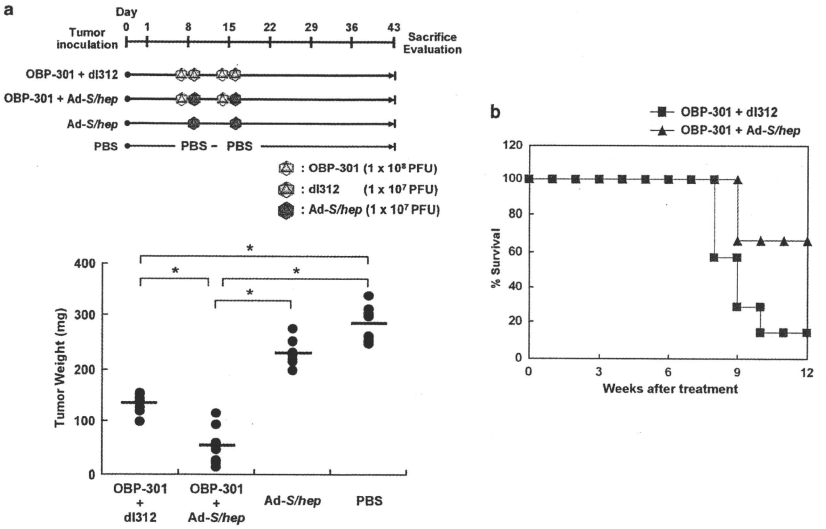

Figure 6 Enhanced antitumor effect of OBP-301 with Ad-*S/hep* in an orthotopic pleural dissemination model. (**a**) Top panel, treatment schedule. Bottom panel, tumor weight of each tumor nodule found in the thoracic spaces after treatment. Treated mice were killed and assessed for pleural dissemination 43 days after tumor inoculation. Closed circles: individual tumor weights. Bars: mean weight. $*P<0.05$. (**b**) Mice bearing H2452 xenografts in the thoracic spaces received intrathoracic administration of either OBP-301 plus dl312 or OBP-301 plus Ad-*S/hep*. Their post-treatment survival was monitored and plotted as a Kaplan–Meier plot.

to therapeutic modalities such as chemotherapy and radiotherapy. An alternative therapeutic option is the use of gene- and vector-based therapies. MPM is characterized by intrathoracic spread, and it is clinically accessible, making it an attractive target for locoregional delivery of genetically engineered viral agents. Replication-competent viral agents can confer specificity of infection and increase viral spread to neighboring tumor cells. Onyx-015, a conditional replication-competent adenovirus lacking the 55-kDa *E1b* gene, may be an effective treatment for human mesothelioma cells retaining wild-type p53 but lacking $p14^{ARF}$ (Ries *et al.*, 2000; Yang *et al.*, 2000, 2001), the targets of Onyx-015, however, are not general and its clinical trials for various types of human malignancies have been discontinued (Goodrum and Ornelles, 1998). In this study, we showed that intrathoracic administration of telomerase-specific oncolytic viruses induced significant antitumor effects against both pre-established and established pleural dissemination of human MPM. Moreover, we found that co-infection of oncolytic adenoviruses with non-replicative adenovirus expressing an ECM-digestive enzyme, heparanase, resulted in a virus distribution into the deeper areas of tumor spheroids, with substantial tumor weight reduction and enhanced efficacy in an orthotopic *in vivo* mesothelioma model.

For the success of gene- and vector-based therapies, it is critical to develop strategies to improve the vector distribution within tumors *in vivo*. Oncolytic viruses can mediate infected cell death, release viral progeny for propagation of infection and induce resultant lysis of neighboring tumor cells. Therefore, these viruses should have a more profound therapeutic efficacy even without particular therapeutic genes when compared with non-replicative viral vectors. Indeed, as human malignant mesothelioma cells express sufficient telomerase activity as well as CAR (Figure 1), most of the disseminated nodules were imaged with GFP fluorescence by intrathoracic administration of GFP-expressing, telomerase-specific OBP-401 in an orthotopic pleural mesothelioma model, which coincided with histologically confirmed mesothelioma (Figure 3). We have recently shown that this OBP-401-mediated GFP-labeling strategy is extremely sensitive to detect disseminated nodules and applicable for the surgical navigation (Kishimoto *et al.*, 2009). A confocal fluorescent imaging system with fibered microprobes showed that OBP-401 could also identify macroscopically invisible tumor tissues, suggesting that OBP-301 might be able to eliminate microscopic dissemination. In fact, local administration of OBP-301 into the thoracic cavity significantly suppressed the disseminated tumor growth (Figure 4). The treatment immediately after mesothelioma

cell inoculation resembles the state of a minimum residual disease after extended surgical excision. Most of the floating mesothelioma cells could be efficiently treated by locoregional OBP-301 administration, resulting in little disseminated tumor nodule formation. Tumor weights, however, increased gradually as the treatment time was delayed (Figure 4c), suggesting that some additional approaches are required to improve the therapeutic efficacy.

Extracellular matrix is a major barrier to macromolecular transport in the tumor interstitium, but digestive enzymes that degrade ECM may overcome the limited spread of viral agents within tumors. Previous studies have shown that protease that degrades multiple ECM components as well as collagenase that digests fibrillar collagen can mediate a broad distribution of virus particles within tumors, leading to enhanced therapeutic efficacy (Kuriyama *et al.*, 2001; McKee *et al.*, 2006). Non-replicating adenovirus vector expressing the matrix metalloproteinase-8 (MMP-8), which effectively degrades collagen-I, was also able to modify a fibrillar collagen substrate to allow oncolytic virus diffusion into tumors (Cheng *et al.*, 2007). More recent studies have also shown that relaxin-expressing, replication-competent adenovirus could increase the virus distribution and show a profound antitumor effect in mice (Kim *et al.*, 2006; Ganesh *et al.*, 2007). Although the most effective enzyme for the promotion of viral penetration into tumor masses has not been determined, we used heparanase, which has a hydrolytic mechanism to cleave glycosidic bonds in the heparan sulfate component of the ECM (McKenzie, 2007).

The expression of functional heparanase degrades the ECM, which in turn improves the uptake and distribution of biological agents including antibodies and viruses (Eikenes *et al.*, 2004). An advantage of heparanase is that other enzymes that are capable of digesting ECM and basement membrane components (such as MMP-2 and MMP-8) can be subsequently induced after heparanase expression. We reported earlier that the over-expression of the heparanase gene upregulated *MMP-2* mRNA expression in human lung cancer cells (Uno *et al.*, 2001). Arterial injury also increased heparanase activity in vascular endothelial cells, which was associated with MMP-2 and MMP-9 activation (Fitzgerald *et al.*, 1999). Therefore, a more prominent virus infiltration through broad ECM degradation with multiple enzymes can be expected by exogenous heparanase expression. The co-infection of Ad-*S/hep* considerably enhanced OBP-401 virus penetration into the multicellular spheroids, mimicking the *in vivo* biology of tumors (Figure 5b, c). Furthermore, combination therapy with OBP-301 and Ad-*S/hep* in an orthotopic murine model significantly reduced the tumor weights of disseminated plural mesothelioma as compared with tumors from mice treated with OBP-301 alone (Figure 6a), suggesting that heparanase-assisted broad virus distribution could mediate a more profound antitumor effect against human malignant mesothelioma.

Our data indicate that this dual virotherapy may be a promising therapeutic strategy for malignant pleural mesothelioma. However, the over-expression of ECM-digesting enzymes may potentially promote the metastasis of tumor cells. MMPs as well as heparanase were detected in many types of human cancer, and their expression has a very active role in tumor invasion and metastasis. Indeed, targeted inhibition of heparanase expression by antisense complementary DNA transfection showed a significant reduction in the invasive and metastatic properties of tumor cells in an animal model (Uno *et al.*, 2001). Short hairpin RNAs that mediated the attenuation of MMP expression also prevented the progression of human tumor cells *in vivo* (Blackburn *et al.*, 2007). Although there is a risk that the metastatic potential of tumor cells may be increased by heparanase expression, we found that the intrathoracic administration of 10^7 PFU of Ad-*S/hep* alone had no apparent effects on the growth of pleural mesothelioma, indicating that this particular dose of the virus appears to be safe (Figure 6a). In the dual-vector system, the two viral loads can be adjusted according to the function of each virus. We showed earlier that telomerase-specific oncolytic viruses and non-replicative adenovirus-expressing functional genes can successfully work together by determining the optimal doses of vectors (Umeoka *et al.*, 2004; Hioki *et al.*, 2008). A single oncolytic virus vector-expressing relaxin inhibits tumor growth and metastasis, however, it may be impossible to reduce the amount of relaxin expression when high doses of the virus are used. In contrast, our dual-vector system of telomerase-specific oncolytic adenovirus in combination with heparanase-expressing replication-deficient adenovirus can be used safely by a fine adjustment of the optimal doses.

In conclusion, our data clearly indicate that telomerase-specific oncolytic adenoviruses have significant therapeutic potential against human malignant pleural mesothelioma *in vitro* and *in vivo*. Moreover, the addition of heparanase-expressing adenovirus significantly enhanced the virus distribution and the antitumor effects of oncolytic adenoviruses. A phase I, dose-escalation study of telomerase-specific oncolytic adenovirus, OBP-301, is currently underway in the United States to assess the treatment feasibility and to characterize its pharmacokinetics in patients with advanced solid tumors (Fujiwara *et al.*, 2008). Phase II studies of telomerase-specific virotherapy in malignant pleural mesothelioma patients are warranted.

Materials and methods

Cell lines and culture conditions

The human mesothelioma cell lines H2052, H2452, H28 and 211H were purchased from American Type Culture Collection (Manassas, VA, USA). H2052 and H2452 cells were cultured as monolayers in RPMI 1640 medium supplemented with 10% fetal bovine serum, 100 units/ml penicillin and 100 mg/ml streptomycin. H28 and 211 H were routinely propagated in monolayer culture in RPMI 1640 medium supplemented with 10% fetal bovine serum, 1 mM sodium pyruvate, 100 units/ml penicillin and 100 mg/ml streptomycin. The human non-small-cell lung cancer cell line H1299 was also cultured in RPMI

1640 medium supplemented with 10% fetal bovine serum, 100 units/ml penicillin and 100 mg/ml streptomycin. The normal human lung diploid fibroblast cell line WI38 (JCRB0518) was obtained from the Health Science Research Resources Bank (Osaka, Japan) and grown in Eagle's MEM with 10% fetal bovine serum. The normal human lung fibroblast and the human umbilical vascular endothelial cell line (TaKaRa Biomedicals, Shiga, Japan) were cultured according to the vendors' specifications.

Recombinant adenoviruses

OBP-301 is a telomerase-specific replication-compenent adenovirus variant, in which the hTERT promoter element drives the expression of *E1A* and *E1B* genes linked with internal ribosome entry site (Figure 1a). OBP-301 was modified to create OBP-401 for monitoring viral replicationthe *GFP* gene was inserted under the cytomegalovirus promoter into the E3 region to create OBP-401. Ad-*S/hep* is a replication-deficient adenovirus expressing the human *heparanase* gene under the cytomegalovirus promoter. The E1A-deleted adenovirus dl312 was used as the control adenovirus.

Flow cytometric analysis

A total of 2×10^5 cells were labeled with mouse monoclonal anti-CAR (RmcBUpstate Biotechnology, Lake Placid, NY, USA) for 30 min at 4 °C. Then, the cells were incubated with fluorescein isothiocyanate-conjugated rabbit anti-mouse IgG second antibody (Zymed Laboratories, South San Francisco, CA, USA) and analysed by flow cytometry (FACSCalibur, Becton Dickinson, Mountain View, CA, USA). An isotype-matched normal mouse IgG_1 conjugated to fluorescein isothiocyanate (Serotec, Oxford, UK) was used as a control.

Quantitative real-time PCR analysis of hTERT mRNA

Total RNA from the culture cells was obtained by using the RNeasy Mini Kit (Qiagen, Chatsworth, CA, USA). Approximately 0.1 μg of total RNA was used for reverse transcription. Reverse transcription was performed at 22 °C for 10 min and then at 42 °C for 20 min. The *hTERT* mRNA copy number was determined by real-time quantitative reverse transcription–PCR using a LightCycler instrument and a LightCycler DNA TeloTAGGG hTERT Quantification Kit (Roche Molecular Diagnostics, Indianapolis, IN, USA). Data analysis was performed using the LightCycler software. The ratios normalized by dividing the value of untreated cells were presented for each sample.

Cell viability assay

The XTT assay was performed to measure cell viability. Briefly, cells were seeded at 1×10^3 cells/well in 96-well plates 16–20 h before viral infection and infected with OBP-301 at a MOI of 0, 1, 10 or 50 PFU/cell. Cell viability was determined at the indicated times by using a Cell Proliferation Kit II (Roche Applied Science, Mannheim, Germany) according to the manufacturer's protocol.

Fluorescent microscopy

Human mesothelioma cell lines were infected with 10 MOI of OBP-401 *in vitro*. Expression of the *GFP* gene was assessed and photographed using an IX71 fluorescent microscope (Olympus, Tokyo, Japan) at indicated times.

Western blot analysis

H2452 cells were collected by trypsinization and washed twice in cold phosphate-buffered saline. Cells then were dissolved in lysis buffer containing 50 mM Tris–HCl (pH7.5), 150 mM NaCl, 0.5% Triton X-100, and protease inhibitors (0.2 mM phenylmethylsulfonyl fluoride, 0.2 mM 4-(2-aminoethyl)benzenesul-fonylfluoride, 10 μg/ml leupeptin, 10 μg/ml pepstatin, and 1 μg/ml aprotinin).The lysis was performed at 4 °C for 30 min, and then the reaction mixture was centrifuged at 15 000 revolutions per minute. The protein concentration of the supernatant was determined by using the Bio-Rad protein determination method (Bio-Rad, Hercules, CA, USA). Equal amounts (60 μg) of proteins were electrophoresed under reducing conditions on 12% (w/v) polyacrylamide gels. Proteins were electrophoretically transferred to Hy-bond-polyvinylidene difluoride transfer membranes (Amersham, Arlington Heights, IL, USA) and incubated with primary antibodies against heparanase or β-actin, and then peroxidase-linked secondary antibody. An enhanced chemiluminescence Western system (Amersham, Tokyo, Japan) was used to detect secondary probes.

Spheroid culture

Single-cell suspensions of H2452 cells were obtained by trypsinization of monolayer cultures that consisted of 1×10^4 cells seeded on SUMILON Celltight Spheroid (Sumitomo Bakelite Co, Tokyo, Japan) according to the manufacturer's protocol. After formation of small spheroidal aggregates, 1×10^3 PFU of Ad-*S/hep* or dl312 were added to the culture, followed by the addition of 1×10^4 PFU of OBP-401 48 h later. The GFP expression in each tumor spheroid was assessed under the laser-scanning confocal fluorescent microscope (Carl Zeiss, Jena, Germany) 48 h later.

Animal experiments

The experimental protocol was approved by the ethics review committee for animal experimentation of our institution. We used a 27-gauge needle to intrathoracically inject female BALB/c *nu/nu* mice with 100 μl of suspension containing 5×10^6 H2452 cells. The same technique was used for each viral injection into the thoracic space at the indicated time points. Mice were killed and their thoracic spaces were examined macroscopically. Tumor nodules in the thoracic spaces were removed and weighted. *In vivo* GFP fluorescence imaging was also acquired by using a Hamamatsu C5810 three-chip color cooled charged-coupled device camera (Hamamatsu Photonics Systems, Hamamatsu, Japan) and an *in situ* molecular imaging system (Cell~VIZIOMauna Kea Technologies, Paris, France).

Statistical analysis

We used the Student's *t*-test to determine statistically significant differences among the groups. *P*-values <0.05 were considered statistically significant.

Conflict of interest

Yasuo Urata is an employee of Oncolys BioPharma, Inc., the manufacturer of OBP-301 and OBP-401. Toshiyoshi Fujiwara is a consultant of Oncolys BioPharma, Inc.

Acknowledgements

We thank for K Nagai for his helpful discussion. We also thank Y Shirakiya, N Mukai, T Sueishi and M Yokota for their excellent technical support. The Cell~VIZIO system was provided by Mauna Kea Technologies (Paris, France).

References

Alberts AS, Falkson G, Goedhals L, Vorobiof DA, Van der Merwe CA. (1988). Malignant pleural mesothelioma: a disease unaffected by current therapeutic maneuvers. *J Clin Oncol* **6**: 527–535.

Ball DL, Cruickshank DG. (1990). The treatment of malignant mesothelioma of the pleura: review of a 5-year experience, with special reference to radiotherapy. *Am J Clin Oncol* **13**: 4–9.

Blackburn JS, Rhodes CH, Coon CI, Brinckerhoff CE. (2007). RNA interference inhibition of matrix metalloproteinase-1 prevents melanoma metastasis by reducing tumor collagenase activity and angiogenesis. *Cancer Res* **67**: 10849–10858.

Chahinian AP, Pajak TF, Holland JF, Norton L, Ambinder RM, Mandel EM. (1982). Diffuse malignant mesothelioma. Prospective evaluation of 69 patients. *Ann Intern Med* **96**: 746–755.

Chailleux E, Dabouis G, Pioche D, de LM, de Lajartre AY, Rembeaux A *et al.* (1988). Prognostic factors in diffuse malignant pleural mesothelioma. A study of 167 patients. *Chest* **93**: 159–162.

Cheng J, Sauthoff H, Huang Y, Kutler DI, Bajwa S, Rom WN *et al.* (2007). Human matrix metalloproteinase-8 gene delivery increases the oncolytic activity of a replicating adenovirus. *Mol Ther* **15**: 1982–1990.

Connelly RR, Spirtas R, Myers MH, Percy CL, Fraumeni Jr JF. (1987). Demographic patterns for mesothelioma in the United States. *J Natl Cancer Inst* **78**: 1053–1060.

Eikenes L, Bruland OS, Brekken C, Davies CL. (2004). Collagenase increases the transcapillary pressure gradient and improves the uptake and distribution of monoclonal antibodies in human osteosarcoma xenografts. *Cancer Res* **64**: 4768–4773.

Fitzgerald M, Hayward IP, Thomas AC, Campbell GR, Campbell JH. (1999). Matrix metalloproteinase can facilitate the heparanase-induced promotion of phenotype change in vascular smooth muscle cells. *Atherosclerosis* **145**: 97–106.

Fujiwara T, Tanaka N, Numunaitis JJ, Senzer NN, Tong A, Ichimaru D *et al.* (2008). Phase I trial of intratumoral administration of OBP-301, a novel telomerase-specific oncolytic virus, in patients with advanced solid cancer: Evaluation of biodistribution and immune response. *J Clin Oncol* **26**: 3572.

Ganesh S, Gonzalez EM, Idamakanti N, Abramova M, Vanroey M, Robinson M *et al.* (2007). Relaxin-expressing, fiber chimeric oncolytic adenovirus prolongs survival of tumor-bearing mice. *Cancer Res* **67**: 4399–4407.

Goodrum FD, Ornelles DA. (1998). p53 status does not determine outcome of E1B 55-kilodalton mutant adenovirus lytic infection. *J Virol* **72**: 9479–9490.

Hioki M, Kagawa S, Fujiwara T, Sakai R, Kojima T, Watanabe Y *et al.* (2008). Combination of oncolytic adenovirotherapy and Bax gene therapy in human cancer xenografted models. Potential merits and hurdles for combination therapy. *Int J Cancer* **122**: 2628–2633.

Kawashima T, Kagawa S, Kobayashi N, Shirakiya Y, Umeoka T, Teraishi F *et al.* (2004). Telomerase-specific replication-selective virotherapy for human cancer. *Clin Cancer Res* **10**: 285–292.

Kim JH, Lee YS, Kim H, Huang JH, Yoon AR, Yun CO. (2006). Relaxin expression from tumor-targeting adenoviruses and its intratumoral spread, apoptosis induction, and efficacy. *J Natl Cancer Inst* **98**: 1482–1493.

Kishimoto H, Kojima T, Watanabe Y, Kagawa S, Fujiwara T, Uno F *et al.* (2006). *In vivo* imaging of lymph node metastasis with telomerase-specific replication-selective adenovirus. *Nat Med* **12**: 1213–1219.

Kishimoto H, Zhao M, Hayashi K, Urata Y, Tanaka N, Fujiwara T *et al.* (2009). *In vivo* internal tumor illumination by telomerase-dependent adenoviral GFP for precise surgical navigation. *Proc Natl Acad Sci USA* **106**: 14514–14517.

Kuriyama N, Kuriyama H, Julin CM, Lamborn KR, Israel MA. (2001). Protease pretreatment increases the efficacy of adenovirus-mediated gene therapy for the treatment of an experimental glioblastoma model. *Cancer Res* **61**: 1805–1809.

McKee TD, Grandi P, Mok W, Alexandrakis G, Insin N, Zimmer JP *et al.* (2006). Degradation of fibrillar collagen in a human melanoma xenograft improves the efficacy of an oncolytic herpes simplex virus vector. *Cancer Res* **66**: 2509–2513.

McKenzie EA. (2007). Heparanase: a target for drug discovery in cancer and inflammation. *Br J Pharmacol* **151**: 1–14.

Molnar-Kimber KL, Sterman DH, Chang M, Kang EH, ElBash M, Lanuti M *et al.* (1998). Impact of preexisting and induced humoral and cellular immune responses in an adenovirus-based gene therapy phase I clinical trial for localized mesothelioma. *Hum Gene Ther* **9**: 2121–2133.

Murayama T, Takahashi K, Natori Y, Kurumatani N. (2006). Estimation of future mortality from pleural malignant mesothelioma in Japan based on an age-cohort model. *Am J Ind Med* **49**: 1–7.

Price B. (1997). Analysis of current trends in United States mesothelioma incidence. *Am J Epidemiol* **145**: 211–218.

Ries SJ, Brandts CH, Chung AS, Biederer CH, Hann BC, Lipner EM *et al.* (2000). Loss of p14ARF in tumor cells facilitates replication of the adenovirus mutant dl1520 (ONYX-015). *Nat Med* **6**: 1128–1133.

Ruffie P, Feld R, Minkin S, Cormier Y, Boutan-Laroze A, Ginsberg R *et al.* (1989). Diffuse malignant mesothelioma of the pleura in Ontario and Quebec: a retrospective study of 332 patients. *J Clin Oncol* **7**: 1157–1168.

Rusch VW, Piantadosi S, Holmes EC. (1991). The role of extrapleural pneumonectomy in malignant pleural mesothelioma. A Lung Cancer Study Group trial. *J Thorac Cardiovasc Surg* **102**: 1–9.

Ryan CW, Herndon J, Vogelzang NJ. (1998). A review of chemotherapy trials for malignant mesothelioma. *Chest* **113**: 66S–73S.

Sterman DH, Recio A, Carroll RG, Gillespie CT, Haas A, Vachani A *et al.* (2007). A phase I clinical trial of single-dose intrapleural IFN-beta gene transfer for malignant pleural mesothelioma and metastatic pleural effusions: high rate of antitumor immune responses. *Clin Cancer Res* **13**: 4456–4466.

Sterman DH, Recio A, Vachani A, Sun J, Cheung L, DeLong P *et al.* (2005). Long-term follow-up of patients with malignant pleural mesothelioma receiving high-dose adenovirus herpes simplex thymidine kinase/ganciclovir suicide gene therapy. *Clin Cancer Res* **11**: 7444–7453.

Sterman DH, Treat J, Litzky LA, Amin KM, Coonrod L, Molnar-Kimber K *et al.* (1998). Adenovirus-mediated herpes simplex virus thymidine kinase/ganciclovir gene therapy in patients with localized malignancy: results of a phase I clinical trial in malignant mesothelioma. *Hum Gene Ther* **9**: 1083–1092.

Taki M, Kagawa S, Nishizaki M, Mizuguchi H, Hayakawa T, Kyo S *et al.* (2005). Enhanced oncolysis by a tropism-modified telomerase-specific replication-selective adenoviral agent OBP-405 ('Telomelysin-RGD'). *Oncogene* **24**: 3130–3140.

Tango Y, Taki M, Shirakiya Y, Ohtani S, Tokunaga N, Tsunemitsu Y *et al.* (2004). Late resistance to adenoviral p53-mediated apoptosis caused by decreased expression of Coxsackie-adenovirus receptors in human lung cancer cells. *Cancer Sci* **95**: 459–463.

Umeoka T, Kawashima T, Kagawa S, Teraishi F, Taki M, Nishizaki M *et al.* (2004). Visualization of intrathoracically disseminated solid tumors in mice with optical imaging by telomerase-specific amplification of a transferred green fluorescent protein gene. *Cancer Res* **64**: 6259–6265.

Uno F, Fujiwara T, Takata Y, Ohtani S, Katsuda K, Takaoka M *et al.* (2001). Antisense-mediated suppression of human heparanase gene expression inhibits pleural dissemination of human cancer cells. *Cancer Res* **61**: 7855–7860.

Yang CT, You L, Uematsu K, Yeh CC, McCormick F, Jablons DM. (2001). p14(ARF) modulates the cytolytic effect of ONYX-015 in mesothelioma cells with wild-type p53. *Cancer Res* **61**: 5959–5963.

Yang CT, You L, Yeh CC, Chang JW, Zhang F, McCormick F *et al.* (2000). Adenovirus-mediated p14(ARF) gene transfer in human mesothelioma cells. *J Natl Cancer Inst* **92**: 636–641.

Supplementary Information accompanies the paper on the Oncogene website (http://www.nature.com/onc)

In Vivo Biological Purging for Lymph Node Metastasis of Human Colorectal Cancer by Telomerase-Specific Oncolytic Virotherapy

Toru Kojima, MD, Yuichi Watanabe, PhD,†‡ Yuuri Hashimoto, BS,†‡ Shinji Kuroda, MD,* Yasumoto Yamasaki, MD,* Shuya Yano, MD,* Masaaki Ouchi, BS,‡ Hiroshi Tazawa, MD, PhD,† Futoshi Uno, MD, PhD,*† Shunsuke Kagawa, MD, PhD,*† Satoru Kyo, MD, PhD,§ Hiroyuki Mizuguchi, PhD,¶ Yasuo Urata, BS,‡ Noriaki Tanaka, MD, PhD,* and Toshiyoshi Fujiwara, MD, PhD*†*

Background/Objective: The aim of this study was to develop a less invasive way of targeting lymph node metastasis for the treatment of human gastrointestinal cancer. Lymphatic invasion is a major route for cancer cell dissemination, and adequate treatment of locoregional lymph nodes is required for curative treatment in patients with malignancies.

Methods: Human telomerase reverse transcription (hTERT) is the catalytic subunit of telomerase, which is highly active in cancer cells but quiescent in most normal somatic cells. OBP-301 (Telomelysin) is an attenuated adenovirus with oncolytic potency that contains the hTERT promoter element to regulate viral replication. We examined whether OBP-301 injected into the primary tumor might be useful for purging micrometastasis from regional lymph nodes in an orthotopic colorectal cancer model.

Results: OBP-301 was intratumorally injected into HT29 tumors orthotopically implanted into the rectum in BALB/c *nu/nu* mice. By using a highly sensitive quantitative PCR analysis that targets the human-specific *Alu* sequence, we showed that OBP-301 caused viral spread into the regional lymphatic area and selectively replicated in neoplastic lesions, resulting in tumor-cell-specific death in metastatic lymph nodes. Moreover, although the surgical removal of primary tumors increased the tendency of lymph node metastasis, preoperative intratumoral injection of virus significantly reduced lymph node metastasis.

Conclusions: Our results indicate that intratumoral injection of OBP-301 mediates effective in vivo purging of metastatic tumor cells from regional lymph nodes, which may help optimize treatment of human cancer, especially gastrointestinal malignancies.

(*Ann Surg* 2010;251: 1079–1086)

From the *Division of Surgical Oncology, Department of Surgery, Okayama University Graduate School of Medicine, Dentistry and Pharmaceutical Sciences, Okayama, Japan; †Center for Gene and Cell Therapy, Okayama University Hospital, Okayama, Japan; ‡Oncolys BioPharma, Inc., Tokyo, Japan; §Department of Obstetrics and Gynecology, Kanazawa University School of Medicine, Kanazawa, Japan; and ¶Department of Biochemistry and Molecular Biology, Graduate School of Pharmaceutical Sciences, Osaka University, Osaka, Japan.

Supported in part by grants from the Ministry of Education, Science, and Culture, Japan (to T. F.); grants from the Ministry of Health and Welfare, Japan (to T. F.).

Supplemental digital content is available for this article. Direct URL citations appear in the printed text and are provided in the HTML and PDF versions of this article on the journal's Web site (www.annalsofsurgery.com).

Reprints: Toshiyoshi Fujiwara, MD, PhD, Center for Gene and Cell Therapy, Okayama University Hospital, 2–5-1 Shikata-cho, Okayama 700–8558, Japan. E-mail: toshi_f@md.okayama-u.ac.jp.

ISSN: 0003-4932/10/25106-1079
DOI: 10.1097/SLA.0b013e3181deb69d

Lymph node status provides important information for both the diagnosis and treatment of human cancer. Lymphatic invasion is a major route for cancer cell dissemination, and lymph node metastasis is a frequent type of recurrence that is associated with a survival disadvantage in many types of cancers.[1–3] Therefore, adequate resection of the locoregional lymph nodes is required for curative treatment in patients with malignancies.[4,5] Extended lymphadenectomy, however, may greatly impair quality of life, especially for patients with early stage epithelial neoplasms in the gastrointestinal tract.[6] Their primary tumors can be removed by new endoluminal therapeutic techniques such as endoscopic submucosal dissection; however, patients with submucosal invasion, lymphovascular infiltration of cancer cells, or undifferentiated histology often become candidates for surgical organ resection with lymphadenectomy, because there is a risk of regional lymph node metastasis, although the frequency is relatively low.[7] Thus, a less invasive way to selectively treat lymph node metastasis would benefit these patients by allowing them to avoid a prophylactic surgery.

Oncolytic viruses that can selectively replicate in tumor cells and lyse infected cells have been extensively investigated as novel anticancer agents.[8–10] These vectors are designed to induce virus-mediated lysis of tumor cells after selective viral propagation within the tumor cell. We previously developed an attenuated adenovirus designated OBP-301 (Telomelysin) that drives the *E1A* and *E1B* genes under the human telomerase reverse transcription (hTERT) promoter.[10–13] The clinical development of OBP-301 as a monotherapy for various solid tumors is currently underway in the United States.[14] We and others have reported that human adenovirus is capable of effective transport into the lymphatic circulation.[15–17] Injection of OBP-401 (TelomeScan), telomerase-specific, replication-competent adenovirus expressing green fluorescent protein (GFP) into primary tumors allows its lymphatic spread, which in turn induces viral replication in metastatic lymph nodes, allowing us to directly image the micrometastases.

In the present study, we explore whether viruses injected into the established primary tumors could traffic to regional lymph nodes and selectively kill metastatic tumor cells in a human colorectal tumor xenograft model. To measure virus-mediated therapeutic efficacy against lymphatic micrometastasis, we established a highly sensitive real-time PCR method targeting human *Alu* sequences.

MATERIALS AND METHODS

Cell Line and Viruses

The human colorectal cancer cell line HT29 was routinely propagated in monolayer culture in McCoy's medium. The recombinant replication-selective, tumor-specific adenovirus vector OBP-301 (Telomelysin), in which the hTERT promoter element drives the expression of *E1A* and *E1B* genes linked with an internal ribosome entry site, was previously constructed and

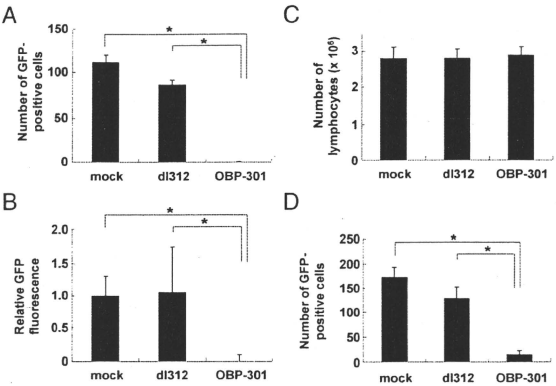

FIGURE 1. In vitro purging effect of OBP-301 infection on HT29 human colorectal cancer cells. We plated 5×10^6 PBMC or mouse splenocytes per well along with 2×10^5 HT29 human colorectal cancer cells. After 24 hours, the mixed culture was infected with 2×10^7 PFU of OBP-301 or dl312 (100 multiplicity of infection [MOI] for HT29 cells) for 96 hours, followed by infection with OBP-401 at 2×10^6 PFU (10 MOI for HT29 cells) to visualize viable HT29 cells (see Figure, Supplemental Digital Content 2, available at: http://links.lww.com/SLA/A39, which illustrates the procedures for in vitro purging experiments). A, The number of GFP-positive, viable HT29 cells was counted in 3 random fields at a magnification of × 200 under the fluorescent microscope. Values represent means ± SEM, and a single asterisk indicates $P < 0.05$ as compared with the other groups. B, The intensity of GFP fluorescence in each treatment group was also measured by using a fluorescence microplate reader. Values are relative to mock (mock = 1) and represent means ± SEM. A single asterisk indicates $P < 0.05$. C, Toxicity of OBP-301 infection was assessed for human lymphocytes. A total of 5×10^6 PBMCs were exposed to 2×10^7 PFU of OBP-301 or dl312 for 96 hours, and their viability was then determined by trypan blue exclusion. D, An efficient purging effect of OBP-301 on HT29 cells in mouse splenocytes. To mimic the animal experiments in vitro, HT29 cells mixed with splenocytes from BALB/c *nu/nu* mice were exposed to OBP-301 or dl312 for 96 hours, followed by OBP-401 infection. The number of cells positive for GFP was counted as described above, and presented as the mean ± SEM. A single asterisk indicates $P < 0.05$.

characterized.[11] OBP-401 (TelomeScan) is a telomerase-specific, replication-competent adenovirus variant in which the replication cassette and *GFP* gene under the control of the cytomegalovirus promoter were inserted into the E3 region for monitoring viral replication[15] (see Figure, Supplemental Digital Content 1, online only, available at http://links.lww.com/SLA/A38, which illustrates schematic DNA structures of telomerase-specific viruses). The *E1A*-deleted adenovirus vector lacking a cDNA insert (dl312) was also used as a control vector.

In Vitro Purging Experiments

For in vitro purging studies, peripheral blood samples were drawn from healthy volunteers, and mononuclear cells were isolated by sedimentation over Ficoll-Hypaque. Mouse spleens were removed aseptically and gently crushed with the flat end of a sterile syringe. The cells were passed through nylon mesh and then placed in buffered ammonium chloride solution to produce osmotic lysis of erythrocytes. We plated peripheral blood mononuclear cells (PBMC) or mouse splenocytes per well along with HT29 cells. The purging effect was assessed with an Eclipse TS-100 fluorescent microscope (Nikon, Tokyo, Japan) by counting the number of GFP-positive cells 24 hours after OBP-401 infection (see Figure, Supplemental Digital Content 2, online only, available at http://links.lww.com/SLA/A39, which illustrates the procedures for in vitro purging experiments). GFP fluorescence was also measured by using a fluorescence microplate reader (DS Pharma Biomedical, Osaka, Japan) with excitation/emission at 485 nm/528 nm.

Xenograft Model of Lymph Node Metastasis

The experimental protocol was approved by the Ethics Review Committee for Animal Experimentation of our institution. The implantation procedures for human rectal cancer xenografts were described previously.[15] Cell suspensions of HT29 cells at a density of 5×10^6 cells in 100 μL of Matrigel (BD Biosciences, Bedford, MA) were slowly injected into the submucosal layer of the rectum by using a 27-gauge needle. For pathologic evaluation of lymph node metastasis, mice were killed and all para-aortic or iliac lymph nodes were isolated and stained with hematoxylin and eosin.

In Vivo Fluorescence Imaging

In vivo GFP fluorescence imaging was acquired by illuminating the animal with a Xenon 150 W lamp. The re-emitted fluorescence was collected through a long pass filter on a Hamamatsu C5810 3-chip color cooled charged-coupled device (CCD) camera (Hamamatsu Photonics Systems, Hamamatsu, Japan). Abdominal images were also obtained during laparotomy with the IVIS CCD camera and analyzed with Living Image 2.20.1 software (Xenogen/Caliper Life Sciences, Hopkinton, MA) for the quantification of lymph node metastasis.

Quantitative Real-Time PCR Analysis

To measure the amounts of human tumor cells in mouse lymph nodes, we applied a previously described quantitative PCR assay that uses primer sets to amplify human *Alu* sequences present in mouse lymph node DNA extracts. Genomic DNA was extracted

from mixed cell cultures or harvested tissues by using a QIAamp DNA Mini Kit (Qiagen Inc., Valencia, CA). To detect human cells in the mouse tissues, a set of human *Alu* primers (sense: 5′-CTG AGG TCA GGA GTT CGA G-3′; and antisense: 5′-TCA AGC GAT TCT CCT GCC-3′) were designed. We performed the quantitative real-time PCR assay by using a LightCycler instrument (Roche Molecular Biochemicals, Indianapolis, IN). PCR amplification began with a 120-second denaturation step at 95°C and then 30 cycles of denaturation at 95°C for 30 seconds, annealing at 63°C for 30 seconds, and extension at 72°C for 30 seconds. We also amplified the mouse *GAPDH* genomic DNA sequence with mouse *GAPDH* primers (sense: 5′-CCA CTC TTC CAC CTT CGA T-3′; and antisense: 5′-CAC CAC CCT GTT GCT GTA-3′) by using the same PCR conditions described for *Alu*. The amounts of *E1A* DNA of OBP-301 and OBP-401 were measured as previously described. The sequences of specific primers used for *E1A* were as follows: sense: 5′-CCT GTG TCT AGA GAA TGC AA-3′; and antisense: 5′-ACA GCT CAA GTC CAA AGG TT-3′. PCR amplification of genomic DNA extracted from mouse lymph nodes was performed with precycling heat activation of DNA polymerase at 95°C for 600 seconds, followed by 40 cycles of denaturation at 95°C for 10 seconds, annealing at 58°C for 15 seconds, and extension at 72°C for 8 seconds. Data analysis was performed with LightCycler Software (Roche Molecular Biochemicals).

Statistical Analysis

We used the Student 2-tailed *t* test to identify statistically significant differences between groups. Results are reported as mean ± SEM. *P* values less than 0.05 were considered statistically significant.

RESULTS

In Vitro Purging of Human Colorectal Cancer Cells by Telomerase-Specific Oncolytic Adenovirus

To examine whether telomerase-specific oncolytic adenovirus can selectively kill human tumor cells among the millions of lymphocytes in lymph nodes, HT29 human colorectal cancer cells were mixed with PBMC from healthy donors and purged in vitro with OBP-301 for 3 days. Viable HT29 cells were then visualized with GFP fluorescence by OBP-401 infection for 24 hours (see Figure, Supplemental Digital Content 2, online only, available at http://links.lww.com/SLA/A39, which illustrates the procedures for in vitro purging experiments). No GFP-positive viable HT29 cells were detected at 3 days postpurging with OBP-301, whereas infection with replication-deficient control adenovirus dl312 had no significant effects on the viability of HT29 cells (Fig. 1A) (see Figure, Supplemental Digital Content 2, online only, available at: http://links.lww.com/SLA/A39, which demonstrates in vitro purging effect of OBP-301 infection). The purging efficacy of OBP-301 was also confirmed by measuring the relative GFP expression of samples by using a fluorescence microplate reader (Fig. 1B). Neither OBP-301 nor dl312 infection affected the viability of PBMC, confirming the safety of OBP-301 to normal human lymphocytes (Fig. 1C). Next, we determined if human tumor cells mixed with mouse lymphocytes obtained from the spleen would be sensitive to OBP-301 treatment. As expected, purging with OBP-301 significantly reduced the number of viable HT29 cells in mouse splenocytes compared with mock- or dl312-treated samples (Fig. 1D).

In Vivo Lymphatic Spread of Virus on Regional Lymph Nodes

To verify that oncolytic adenoviruses traffic through the lymphatics to the regional lymph nodes, we used an orthotopic mouse model of human rectal cancer with spontaneous lymph node metastasis. We first determined whether the regional lymphatic system, including lymphatic vessels and lymph nodes, could be assessed by injecting dye into the primary tumors. Intense blue staining was detected in regional lymph nodes as early as 1 minute after injection of indigo carmine blue dye into the primary rectal tumors, indicating that the injected solution could rapidly enter the intratumoral lymphatics, which provides a route from the primary tumor to draining lymph nodes (Fig. 2A). Five days after OBP-401 injection into the primary tumors, we also detected GFP expression in both primary rectal tumors and metastatic lymph nodes under the laparotomy by using a 3-chip CCD optical imaging system (Fig. 2B).

To further evaluate the selective replication ability of telomerase-specific oncolytic adenovirus in metastatic lymph nodes, we measured the relative amounts of *E1A* DNA by quantitative real-time PCR analysis. The metastatic GFP-positive lymph nodes con-

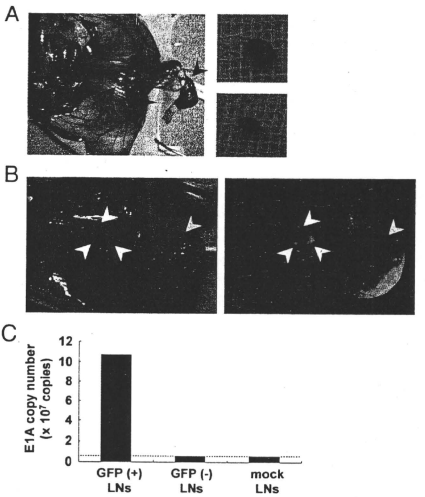

FIGURE 2. In vivo lymphatic spread of virus on regional lymph nodes. A, A lymphatic drainage pattern in an orthotopic xenograft of human HT29 cells. The abdominal cavity was photographed 1 minute after injection of 1% indigo carmine blue dye into an established orthotopic HT29 tumor. Arrowheads indicate the lymph nodes stained with blue dye. Gross appearance of the abdominal cavity (left) and excised lymph nodes (right). B, Five days after intratumoral injection of 1×10^8 PFU of OBP-401, HT29 tumor-bearing *nu/nu* mice were assessed for lymph node metastasis during laparotomy. Macroscopic (left) and fluorescent (right) images. Primary tumor (yellow arrowhead) and metastatic lymph nodes (white arrowheads) are shown. C, Assessment of viral replication in metastatic lymph nodes. GFP-positive and -negative lymph nodes were harvested from mice with HT29 tumor xenografts 5 days after injection of 1×10^8 PFU of OBP-401 and then subjected to real-time quantitative PCR assay to quantify the amounts of viral *E1A* copy number. The value in mock-infected lymph nodes is indicated with a dotted line as a baseline level.

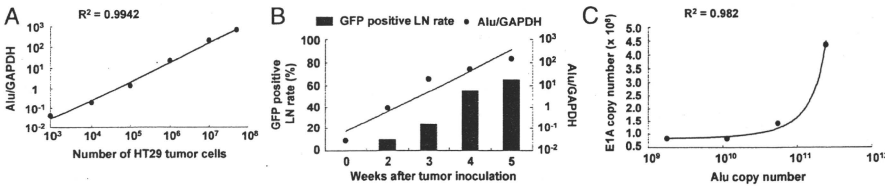

FIGURE 3. Detection and quantification of human cancer cells in mouse tissues with a quantitative real-time *Alu*PCR analysis. A, Generation of a standard curve. Mouse splenocytes (5×10^7 cells) were spiked with serially diluted HT29 human colorectal cancer cells. Genomic DNA was extracted from the mixtures and then subjected to the quantitative amplification (see Figure, Supplemental Digital Content 4A, available at: http://links.lww.com/SLA/A41, which illustrates schematic procedures of detection and quantification of human cancer cells in mouse splenocytes). The *Alu*/*GAPDH* ratios *versus* the numbers of spiked HT29 cells are presented. Regression analysis yielded a correlation coefficient of $R^2 = 0.9942$. The data are representative of 3 separate experiments. B, Quantitative analysis of spontaneous lymph node metastasis. Genomic DNA was extracted from the lymph nodes of mice bearing human HT29 tumor xenografts at the indicated time points after tumor inoculation and analyzed with the quantitative *Alu*PCR assay (see Figure, Supplemental Digital Content 4B, available at: http://links.lww.com/SLA/A41, which illustrates schematic procedures of detection and quantification of human cancer cells in mouse tissues). Metastatic lymph nodes were simultaneously visualized by injecting 1×10^8 PFU of OBP-401 into the primary tumors 5 days before lymph node isolation. C, The viral *E1A* copy numbers were also determined in genomic DNA extracted from isolated lymph nodes by the quantitative real-time PCR method and plotted *versus* the *Alu* copy numbers.

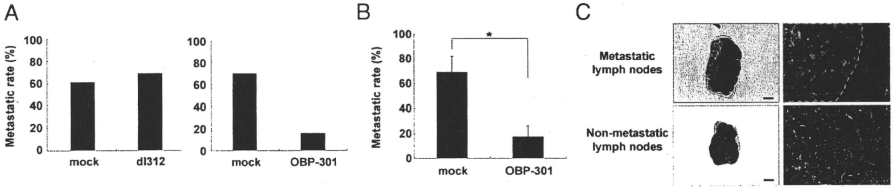

FIGURE 4. Histologic evaluation of selective antitumor effect of OBP-301 delivered into primary tumors on lymphatic metastasis in a colorectal cancer xenograft model. Mice bearing orthotopic HT29 tumors received 3 courses of intratumoral injections of 1×10^8 PFU of OBP-301 or dl312 every 2 days beginning on day 14 after the tumor inoculation. A, On day 35, we harvested a total of 23 to 29 lymph nodes from 5 to 8 mice per group, stained them with hematoxylin and eosin, and calculated metastatic rates. B, In a separate experiment, metastatic rates were histologically determined in individual mice and averaged with S.E.M. ($n = 8$). A single asterisk denotes statistical significance ($P < 0.05$) as compared with the mock group. C, Paraffin-embedded sections of lymph nodes with or without metastatic foci were obtained 35 days after tumor cell implantation and stained with hematoxylin and eosin. Left, ×40 magnification; right, ×200 magnification. Scale bar, 100 μm. The area with metastatic HT29 cells is indicated with the green dotted line.

tained more than 10^8 copies of OBP-401, whereas the number of viral genomes was at the baseline level in nonmetastatic GFP-negative lymph nodes (Fig. 2C). The trafficking and replication ability of the virus was also confirmed in an orthotopic head and neck cancer xenograft model (see Figure, Supplemental Digital Content 3, online only, available at: http://links.lww.com/SLA/A40, which demonstrates OBP-401 virus spread delivered into primary tumors).

Establishment of Highly Sensitive Quantitative Detection Assay for Lymph Node Metastasis

To achieve the highest sensitivity for detecting metastatic human tumor cells in mouse lymph nodes, we applied a novel quantitative real-time PCR assay that uses primer sets to amplify the consensus human *Alu* sequence.[18–20] *Alu* repeat sequences are specific to all human cells and are completely absent in mouse tissues.[21] To test the sensitivity and range of the assay, mouse splenocytes obtained from athymic *nu*/*nu* mice were spiked with variable numbers of HT29 human colorectal cancer cells in vitro (see Figure, Supplemental Digital Content 4A, online only, available at: http://links.lww.com/SLA/A41, which illustrates schematic procedures of detection and quantification of human cancer cells in mouse splenocytes). The total genomic DNA was extracted from the mixtures and subjected to quantitative *Alu*PCR. We also used the human *GAPDH* gene as an internal control to normalize the *Alu* signal in each sample. By plotting the *Alu*/*GAPDH* ratio as a function of the number of spiked tumor cells, a standard curve could be generated with a linear range between 10^3 and 10^8 cells, and regression analysis of the *Alu*/*GAPDH* ratio *versus* the number of expected tumor cells yielded a correlation coefficient of $R^2 = 0.9942$ ($P < 0.01$) (Fig. 3A). These results suggest that the *Alu*/*GAPDH* ratio reflects the actual human tumor cells among mouse splenocytes.

To verify the accuracy and sensitivity of the assay in vivo, we extracted DNA from total lymph nodes at different time points after the orthotopic implantation of HT29 cells and subjected the DNA to the *Alu*PCR analysis (see Figure, Supplemental Digital Content 4B,

online only, available at: http://links.lww.com/SLA/A41, which illustrates schematic procedures of detection and quantification of human cancer cells in mouse tissues). Then, we compared the *Alu/GAPDH* ratios and the metastatic rates determined with GFP expression by injection of OBP-401 into the primary rectal tumors 5 days before lymph node isolation. The *Alu/GAPDH* ratio showed a linear increase in a time-dependent manner, as the GFP-positive metastatic lymph node rate gradually increased (Fig. 3B). By calculating the estimated number of tumor cells according to the standard curve, we also demonstrated the time-dependent logarithm increase in metastatic human tumor cells in mouse lymph nodes (see Figure, Supplemental Digital Content 5, online only, available at: http://links.lww.com/SLA/A42, which demonstrates quantitative analysis of time-dependent development of spontaneous lymph node metastasis). Moreover, when HT29 tumor-bearing mice received a single intratumoral injection of OBP-401, the number of *Alu* copies was clearly correlated with the number of *E1A* copies in isolated mouse lymph nodes ($R^2 = 0.982$, $P < 0.01$), because telomerase-specific oncolytic adenovirus replicates only in metastatic tumor cells (Fig. 3C).

Histologic Evaluation of the In Vivo Antitumor Effect of Virus on Lymph Node Metastasis

We next examined the in vivo antitumor effect of OBP-301 injected into the primary tumors on the regional lymph node metastasis. Mice bearing orthotopic HT29 rectal tumors with a diameter of 7 to 10 mm received 3 courses of intratumoral injections of 10^8 plaque forming units (PFU) of OBP-301 or dl312, or PBS (mock treatment), every 2 days beginning on day 14 after the tumor inoculation. Histopathological examination of the excised total lymph nodes on day 35 showed that OBP-301 treatment considerably reduced the metastatic rates compared with that of mock-treated group, although replication-deficient dl312 had no apparent effects (Fig. 4A) (see Table, Supplemental Digital Content 6, online only, available at: http://links.lww.com/SLA/A43, which demonstrates histologic evaluation of antitumor effect of OBP-301 on lymph node metastasis). We also confirmed that OBP-301 significantly lowered the lymph node metastatic rates by averaging the histologically determined metastasis rates in individual mice ($P < 0.05$) (Fig. 4B). Representative histopathological images of lymph nodes with or without metastatic foci composed of HT29 tumor cells are shown in Figure 4C.

Quantitative Evaluation of the In Vivo Antitumor Effect of Virus on Lymph Node Metastasis

By using a highly sensitive quantitative *Alu*PCR assay, we next investigated the antitumor effect of OBP-301 injected into the primary tumors on lymph node metastasis, which might be histopathologically undetectable. Mice received 3 courses of injections of 10^8 PFU of OBP-301, 10^8 PFU of dl312, or PBS (mock treatment) into orthotopic HT29 rectal tumors every 2 days beginning on day 14 after tumor inoculation. The *Alu* real-time PCR assay of isolated lymph nodes on day 35 demonstrated that mice treated with OBP-301 exhibited significantly fewer metastatic tumor cells as compared with dl312- or mock-treated mice (Fig. 5A). A more profound antitumor effect was achieved by increasing the number of injection cycles from 3 to 5 (see Figure, Supplemental Digital Content 7, online only, available at: http://links.lww.com/SLA/A44, which demonstrates quantitative analysis of antitumor effect of OBP-301 on lymph node metastasis). As expected, regional lymph nodes obtained from OBP-301-treated mice contained more *E1A* copies than the lymph nodes of mock-treated mice (Fig. 5B), suggesting that intratumorally delivered OBP-301 could spread and selectively replicate in metastatic lymph nodes.

We also used OBP-401 and the IVIS imaging system to assess the in vivo antitumor effect of OBP-301 on lymph node metastasis. After 14 days of orthotopic implantation of HT29 cells, OBP-301 (1×10^8 PFU/body) was administered intratumorally for 5 cycles. We then used the IVIS imaging system to explore the abdominal cavity at laparotomy on day 35 following a single injection of OBP-401 (1×10^8 PFU/body) into HT29 rectal tumors on day 30 (see Figure, Supplemental Digital Content 8, online only, available at: http://links.lww.com/SLA/A45, which illustrates schematic procedures of quantitative imaging of lymph node metastasis by the IVIS system). The number of GFP-positive lymph nodes and the GFP signal levels of individual lymph nodes were much higher in mock-treated control mice than in OBP-301-treated mice (Fig. 6A). Indeed, the sum of GFP fluorescence intensity in the abdominal cavity was significantly lower in mice treated with OBP-301 as compared with the mock-treated group, confirming the in vivo biologic purging effect of OBP-301 (Fig. 6B).

Preoperative Purging Efficacy of Oncolytic Virotherapy against Lymph Node Metastasis

To compare the local control rates of virotherapy and radiotherapy for lymph node metastasis, mice bearing orthotopic HT29 tumors were treated with an intratumoral injection of 10^8 PFU of

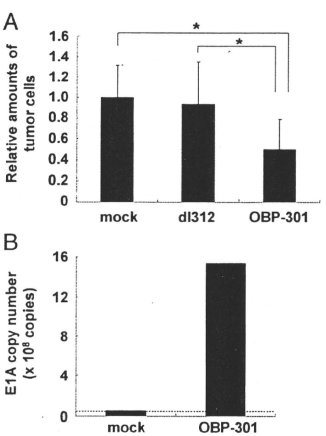

FIGURE 5. Quantitative PCR analysis of the antitumor effect of OBP-301 on lymph node metastasis in an orthotopic colorectal cancer xenograft model. A, Mice with established orthotopic HT29 tumors were treated with intratumoral injection of 1×10^8 PFU of OBP-301 or dl312 every 2 days for 3 cycles starting on day 14 after tumor inoculation. Lymph nodes were harvested on day 35, and then DNA was extracted and subjected to the quantitative *Alu*PCR analysis. The number of metastatic tumor cells is defined as the *Alu/GAPDH* ratio relative to that of the mock-treated sample (mock = 1). Data are shown as the mean ± SEM of 3 separate experiments. Statistical significance was defined as $P < 0.05$ (single asterisk). B, Genomic DNA extracted from lymph nodes of mice that received OBP-301 or PBS was also analyzed with real-time PCR targeting *E1A* to quantify the viral replication. A dotted line represents the baseline level.

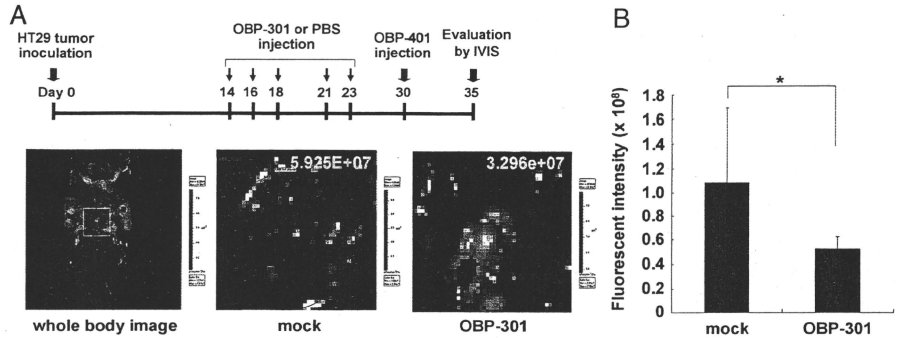

FIGURE 6. Quantitative imaging of lymph node metastasis to evaluate the antitumor effect of OBP-301 in an orthotopic colorectal cancer xenograft model. A, Quantitative imaging of lymph node metastasis by the IVIS system. Mice bearing HT29 xenograft tumors were treated with 5 cycles of intratumoral delivery of 1×10^8 PFU of OBP-301, followed by injection of OBP-401 (10^8 PFU) into HT29 tumors. Five days later, mice were killed and GFP expression was quantitated at laparotomy by IVIS camera (see Figure, Supplemental Digital Content 8, available at: http://links.lww.com/SLA/A45, which illustrates schematic procedures of quantitative imaging of lymph node metastasis by the IVIS system). B, GFP expression was measured as the mean photon flux in mock- and OBP-301-treated groups. A single asterisk indicates a statistically significant difference as compared with the mock-treated group.

OBP-301 or lower hemi-body ionizing radiation at a dosage of 3.3 Gy every 2 days for 3 cycles starting 14 days after tumor inoculation (see Figure, Supplemental Digital Content 9, online only, available at: http://links.lww.com/SLA/A46, which illustrates schematic procedures of quantitative PCR evaluation). The *Alu*PCR analysis of isolated lymph nodes at day 35 demonstrated that both intratumoral administration of OBP-301 and radiation equally resulted in a significant suppression of lymph node metastasis compared with mock-treated mice (Fig. 7A). However, regarding the adverse effects, the lower hemi-body irradiation targeting the regional paraaortic lymph nodes induced a significant body weight loss in mice approximately 10 to 14 days after treatment, whereas there were no apparent adverse effects in mice injected with OBP-301 during the observation period (data not shown). These results suggest that oncolytic virotherapy is less toxic than regional radiotherapy, although the antitumor effects of both approaches may be equivalent.

Finally, we examined whether preoperative intratumoral administration of OBP-301 had an antitumor effect against lymph node metastasis following the primary tumor resection. Mice bearing orthotopic HT29 tumors received intratumoral injections of 10^8 PFU of OBP-301 every 2 days for 3 cycles starting 10 days after tumor inoculation. After primary rectal tumors were surgically removed on day 15, regional para-aortic lymph nodes were isolated on day 35, and then subjected to the *Alu*PCR analysis (see Figure, Supplemental Digital Content 9, online only, available at: http://links.lww.com/SLA/A46, which illustrates schematic procedures of quantitative PCR evaluation). The surgical resection of primary tumors caused considerable enhancement of lymph node metastasis; the preoperative treatment with OBP-301, however, not only inhibited the increase of lymphatic metastasis, but also significantly reduced lymph node metastasis compared with mock-treated mice (Fig. 7B). Images of representative mice before and after primary tumor resection are shown in Figure 7C. As implanted HT29 cells formed submucosal tumors with a solid architecture, tumors could be successfully excised with an incision in the anorectal wall (Fig. 7D).

DISCUSSION

Lymph node metastases represent an aggressive tumor behavior and are associated with a high rate of regional recurrence, which portends a poor outcome and may produce marked morbidity.[1–3] Therefore, it would be clinically beneficial to eliminate or prevent lymph node metastasis to yield a better prognosis for cancer patients. Despite advances in surgical procedures of extended lymphadenectomy,[4,5] a more effective and less invasive management of lymphatic metastasis is needed. Here we describe a new, simple, and robust strategy that uses the telomerase-specific, replication-selective, oncolytic adenovirus OBP-301 to suppress tumor cell dissemination to regional lymph nodes in an orthotopic human colorectal cancer xenograft model.

The therapeutic potential of viral agents against primary tumors as well as their systemic biodistribution targeting distant metastases has been intensively investigated.[8,9,22] Few studies, however, have examined the ability of the virus to traffic to the regional draining lymph nodes. Recently, Burton et al showed that replication-deficient adenovirus could be successfully transported to the regional lymph nodes and noninvasively detect metastasis by expressing the prostate-specific reporter gene in an orthotopic prostate xenograft.[17] We have also previously demonstrated that intratumoral injection of the telomerase-specific, replication-selective, GFP-expressing adenovirus OBP-401 could efficiently visualize metastatic lymph nodes with GFP fluorescence signals in human cancer xenograft models.[15,23] Although these previous studies suggest the possible application of the adenovirus vectors as a lymphotropic agent for the treatment of lymph node metastasis, this effect has not been tested prior to the present study.

In vitro purging experiments demonstrated that OBP-301 infection could selectively eliminate human tumor cells in the presence of human or mouse lymphocytes (Fig. 1). We used OBP-401 to visualize viable human tumor cells after purging with OBP-301, as we have previously shown the high sensitivity and specificity

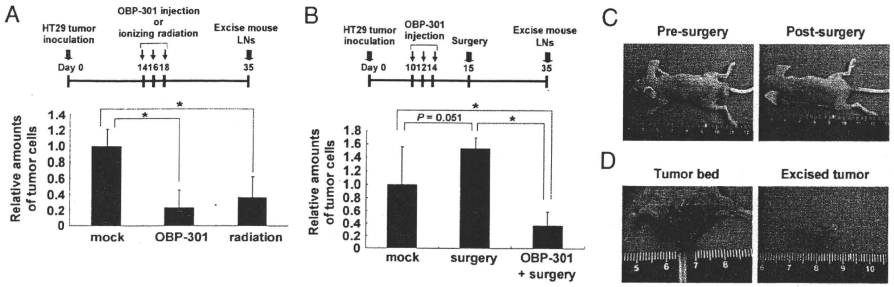

FIGURE 7. Comparative analysis of OBP-301 virotherapy with radiotherapy and surgery. A, In vivo purging effects of regional therapy with OBP-301 or ionizing irradiation on lymph node metastasis. Mice bearing HT29 xenograft tumors received 3 cycles of either intratumoral administration of OBP-301 (10^8 PFU) or lower hemibody irradiation starting at day 14 after tumor inoculation. Radiation was given every 2 days in 3.3-Gy fractions for a total dose of 10 Gy/mouse (see Figure, Supplemental Digital Content 9, available at: http://links.lww.com/SLA/A46, which illustrates schematic procedures of quantitative PCR evaluation). The number of metastatic tumor cells in mouse lymph nodes isolated on day 35 is defined as the *Alu*/*GAPDH* ratio relative to that of the mock-treated sample (mock = 1). Data are shown as the mean ± SEM of 3 separate experiments. Statistical significance was defined as $P < 0.05$ (single asterisk). (B) Preoperative purging effect of OBP-301 on lymph node metastasis. HT29 tumor-bearing mice were intratumorally injected with either 10^8 PFU of OBP-301 or PBS on days 10, 12, and 14 after tumor inoculation. Primary HT29 tumors were surgically removed on day 15. The relative amount of HT29 tumor cells in mouse lymph nodes isolated on day 35 was assessed by the *Alu*PCR assay (see Figure, Supplemental Digital Content 9, available at: http://links.lww.com/SLA/A46, which illustrates schematic procedures of quantitative PCR evaluation). Note that the preoperative intratumoral administration of OBP-301 significantly (single asterisk: $P < 0.05$) reduced the number of metastatic tumor cells as compared with untreated or surgically treated mice. C, External images of orthotopic HT29 tumor-bearing *nu/nu* mice before and after surgical removal of the primary tumor. D, Macroscopic appearance of the tumor bed after surgical resection of the primary tumor, and the excised HT29 tumor.

of this molecular imaging method.[15,23] It has been reported that the fiber-modified adenovirus serotype 5 (Ad5) and the adenovirus vector based on another serotype such as 35 efficiently transduce exogenous genes into hematopoietic cells, including stem cells; the unmodified Ad5, however, could rarely infect these cells because of the lack of the coxsackievirus and adenovirus receptor expression.[24] Indeed, Ad5-based OBP-301 had no apparent effects on the viability of lymphocytes in vitro. These results suggest that normal lymphocytes in the regional lymph nodes could be strictly protected from OBP-301-induced oncolysis, because lymphocytes are not permissive for OBP-301 infection and viral replication is also unlikely to occur in normal cells due to their low telomerase activity.[25]

Previously, we used serial tissue sections of mouse lymph nodes stained with hematoxylin and eosin to detect microscopic metastasis; this time-consuming technique, however, is not quantitative.[15,23] To quantify the few metastatic human tumor cells in a background of large numbers of mouse host cells, a simple real-time *Alu*PCR assay was developed in the current study. This human-specific amplification method enabled us to detect human tumor cells in a linear range of 10^3 to 10^8 cells/sample and monitor the time-dependent exponential growth of spontaneous lymph node metastasis from orthotopic colorectal tumor xenografts (Fig. 3). In accordance with the histologically confirmed results, the *Alu*PCR assay indicated that intratumoral injection of OBP-301 into the primary tumors significantly inhibited lymph node metastasis with high levels of viral replication (Figs. 4, 5). We also used the previously established OBP-401-mediated in vivo imaging in combination with a 3-dimensional optical detection system (IVIS 200) to demonstrate a significant suppressive effect of OBP-301 against lymph node metastasis (Fig. 6). The fact that 2 independent and highly sensitive approaches showed comparable results suggests a potent in vivo purging effect of oncolytic virotherapy on regional lymph nodes.

Currently, surgery and radiation are the most effective and clinically reliable local management strategies for human malignancies including lymphatic metastases. Indeed, ionizing radiation targeting the lower half of the mouse body including primary tumors and the para-aortic lymphatic area significantly inhibited lymph node metastasis (Fig. 7A), although the systemic toxicity such as the body weight loss was remarkable in irradiated mice compared with mice treated with OBP-301 (data not shown). In fact, a total body irradiation at a dose of 10 Gy has been reported to be lethal in mice because of acute radiation syndromes involving the hematopoietic system and gastrointestinal tract.[26] In this regard, our data clearly indicate that regional oncolytic virotherapy might be more simple and safe than radiotherapy as a treatment for metastatic lymph nodes. We also assessed the effect of surgical resection of primary rectal tumors on lymph node metastasis. Unexpectedly, metastatic tumor cells in the lymph nodes considerably increased after surgical removal of primary tumors, presumably due to the excessive load to the host. Another possible explanation of this phenomenon includes a decrease in angiogenic inhibitors such as angiostatin and endostatin secreted from the primary tumor mass.[27] In contrast, intratumoral injection of OBP-301 prior to surgical resection significantly inhibited lymph node metastasis (Fig. 7B), suggesting that, although the surgical procedure itself has the potential to promote regional metastasis, the preoperative treatment with OBP-301 may prevent this undesirable event.

CONCLUSION

The highly sensitive PCR assay targeting the human *Alu* sequence has shown that the oncolytic adenovirus delivered to the